

Improved Lunar Irradiance Model Using Multiyear MODIS Lunar Observations

Junqiang Sun^{ID} and Xiaoxiong Xiong^{ID}

Abstract—The Moderate Resolution Imaging Spectroradiometer (MODIS) instruments on board the Terra and Aqua space-crafts were launched on December 18, 1999, and May 4, 2002, respectively. One of the features of the MODIS instruments is the ability to perform observations of the lunar surface from its space view (SV) port. This event is scheduled approximately once a month via a spacecraft roll maneuver, which enables the lunar phase to be confined to within 1° for each instrument. The Moon is considered to be an extremely stable reference to monitor the long-term radiometric stability of the reflective solar bands (RSB). Each MODIS instrument can also view the Moon for about four months in a year without a roll maneuver. This is caused by the intrusion of the Moon in the SV. The lunar phase angles of these unscheduled lunar observations are distributed over a wide range varying from approximately 50° to 80° for Terra MODIS and from about -80° to -50° for Aqua MODIS, where the positive phase angle refers to a waning Moon, while the negative phase angle corresponds to a waxing Moon. Together, the scheduled and unscheduled lunar observations are used to monitor the long-term radiometric stability of the RSB. Of the several challenges involved in the modeling of the lunar optical properties, such as its absolute brightness, a number of optical and view geometry effects need to be considered. These effects are much easier to characterize for the scheduled observations due to confinement of the lunar phase angles compared to those for the unscheduled intrusions of the Moon in the SV. Nevertheless, it is still a challenge to remove the view geometry effect in the calibration coefficients derived from the scheduled lunar observations and even more challenging for the unscheduled lunar intrusions. In this work, the lunar absolute irradiance is modeled using known attributes and from the lunar observations by the two MODIS instruments from the time period between the years 2005 and 2012. The model developed here attempts to mitigate for the deficiencies in the lunar irradiance measurements by the RObotic Lunar Observatory (ROLO) model, developed by the United States Geological Survey. Overall, the relative uncertainty of the ROLO model for MODIS calibration has been assessed to be about 4% for the shortest wavelength (a center wavelength of 412 nm) in the phase angle range mentioned above. With our new established lunar model, the calibration coefficients derived from the lunar observations, especially those from the unscheduled lunar observations, for the RSB of the two MODIS instruments are significantly improved for the entire mission. A good agreement is observed between the calibration coefficients

derived from the scheduled and unscheduled lunar observations. Both the absolute uncertainty of the new lunar irradiance model and its relative uncertainty due to view geometry variation are much smaller than those of the current ROLO model which has been widely used for most remote sensors' lunar calibrations. Our newly developed lunar irradiance model can be applied to other remote sensors for their lunar calibrations as well. Finally, the significant improvement in the measurement of the lunar irradiance led to a polarization effect in the Moon response for MODIS to be identified. In this article, the impact of the polarization of the moonlight for the MODIS RSB is quantified. This is extremely vital as polarization effect for remote sensors such as MODIS and the follow-on suite of the Joint Polar Satellite System Visible Infrared Imaging Radiometer Suite has been found to significantly increase the calibration uncertainty, especially at short wavelengths.

Index Terms—Calibration, radiometry, remote sensing.

I. INTRODUCTION

THE Moderate Resolution Imaging Spectroradiometer (MODIS) instruments on board the Terra and Aqua space-crafts have been on-orbit for more than 20 and 18 years since their launch, respectively [1]–[4]. Fig. 1 shows a schematic of the instrument. MODIS has 36 spectral bands, among which 20 are reflective solar bands (RSBs) covering a spectral range from 0.41 to 2.2 μm at three resolutions and different numbers of detectors [1]–[4]. The band-related information and center wavelengths of the MODIS RSB are listed in Table I. The RSB is calibrated on-orbit by an on-board solar diffuser (SD), whose degradation is tracked by a solar diffuser stability monitor (SDSM) [3], [4]. Each MODIS instrument has also been scheduled to view the Moon approximately monthly through its space view (SV) port, primarily used to provide the instrument dark response, to track the RSB on-orbit gain changes [5], [6]. MODIS has a two-sided scan mirror that samples the on-board calibrators and the Earth view (EV) continuously with a scan period of 1.477 s. The RSB views the SD and the SV (the Moon) at different angle of incidence (AOI) on the scan mirror and thus, the SD and lunar calibrations track the RSB degradation at two different AOIs.

For each of the MODIS instruments, the response versus scan angle (RVS) of its scan mirror has been found to significantly change on-orbit with time, especially at short wavelengths, and the changes are both time and AOI dependent [7]. In other words, the RSB gains degrade differently at different AOIs of the scan mirror. In early mission, the RVS on-orbit change with the AOI was described by a linear

Manuscript received July 24, 2019; revised November 20, 2019 and June 19, 2020; accepted July 21, 2020. This work was supported by the NASA MODIS Calibration Funding. (*Corresponding author:* Junqiang Sun.)

Junqiang Sun is with Science Systems and Applications, Inc., Lanham, MD 20706 USA (e-mail: junqiang.sun@ssaihq.com).

Xiaoxiong Xiong is with Science Exploration Directorate, NASA Goddard Space Flight Center (NASA/GSFC), Greenbelt, MD 20771 USA (e-mail: xiaoxiong.xiong-1@nasa.gov).

Color versions of one or more of the figures in this article are available online at <http://ieeexplore.ieee.org>.

Digital Object Identifier 10.1109/TGRS.2020.3011831

0196-2892 © 2020 IEEE. Personal use is permitted, but republication/redistribution requires IEEE permission.

See <https://www.ieee.org/publications/rights/index.html> for more information.

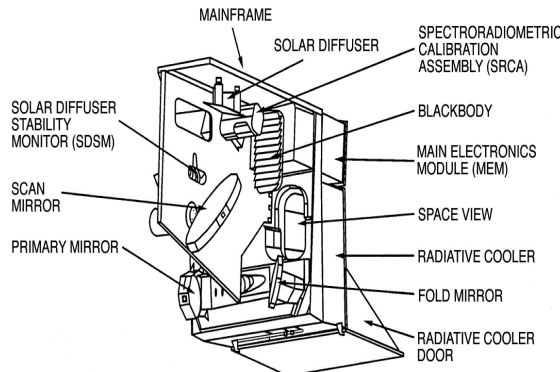


Fig. 1. Schematic for the MODIS instrument.

TABLE I
CENTER WAVELENGTH, NUMBER OF DETECTORS, NUMBER
OF SUBFRAMES, AND SPATIAL RESOLUTION
FOR THE MODIS RSB

Band	Wavelength (nm)	Number of Detectors	Number of Subframes	Resolution (Meter)
1	645	40	4	250
2	858	40	4	250
3	469	20	2	500
4	555	20	2	500
5	1240	20	2	500
6	1640	20	2	500
7	2130	20	2	500
8	412	10	1	1000
9	443	10	1	1000
10	488	10	1	1000
11	531	10	1	1000
12	551	10	1	1000
13	667	10	1	1000
14	678	10	1	1000
15	748	10	1	1000
16	869	10	1	1000
17	905	10	1	1000
18	936	10	1	1000
19	940	10	1	1000
26	1375	10	1	1000

approximation and then the change was derived from the SD and lunar calibrations [5]. After the six-year design lifetime, the RVS on-orbit change can no longer be described by a linear approximation or even higher order polynomials using measurements only from its on-board calibrators. As a result, the RSB gains at multiple AOIs are required to determine the RVS on-orbit changes, especially for short-wavelength bands (comprises bands 3, 4, and 8–12). To obtain these gains, so-called “pseudo-invariant” desert sites [8] are used to track instrument response trending at multiple AOIs [7].

The Moon is known to be an excellent radiometric reference in the visible and near-infrared spectral regions. This enables the lunar-based gain changes at the SV AOI for the RSB to be extremely reliable, especially to characterize the long-term changes in the instrument’s radiometric characteristics. The SD calibration has a known long-term bias due to its nonuniform degradation with respect to the incident and outgoing directions [9]. The “pseudo-invariant” desert sites [8] may not

be as stable as the Moon and, thus, the gains derived from the measurements of the desert sites have a larger uncertainty compared to those obtained from the lunar observations. Therefore, lunar calibration plays a very critical and essential role in the RSB on-orbit calibration of the two MODIS instruments. It also plays an important role in other Earth observing system’s remote sensors such as the Suomi National Polar-orbiting Partnership (SNPP) Visible Infrared Imaging Radiometer Suite (VIIRS) [10], [11], NOAA-20 VIIRS [12], and the Sea-Viewing Wide Field-of-View Sensor (SeaWiFS) [13]. Besides tracking the RSB radiometric on-orbit changes, the lunar observations have also been used to track the spatial characterization of the MODIS RSB and as a near-ideal signal source to characterize the crosstalk and optical leak in the thermal emissive bands (TEB), sensor intercomparison, etc. [14]–[19].

As of April 2020, there have been 188 and 174 scheduled lunar observations for Terra MODIS and Aqua MODIS, respectively. In addition, there are numerous unscheduled lunar observations [20], [21]. The Moon can automatically occur in the view of the SV [6]. These events occur over 100 times for each MODIS instrument every year. Compared to the scheduled lunar observations, the phase angles of the unscheduled MODIS lunar observations are distributed over a very large range, requiring an accurate correction for the effect of the view geometry described by Sun–Moon distance, Moon–MODIS distance, lunar phase angle, and lunar librations if these unscheduled lunar observations are applied to track the RSB on-orbit gain changes [20], [21]. Among all the unscheduled lunar observations, only partial of them provide full image of the Moon and only these unscheduled lunar observations can be applied to track the RSB on-orbit changes. So far, there are about 792 and 571 such unscheduled lunar observations for Terra MODIS and Aqua MODIS, respectively. Compared to the scheduled lunar observations, those unscheduled do not require special spacecraft maneuvers and are, therefore, risk-free from instrument’s safety point of view.

The correction of the view geometry effect is very critical for accuracy of the RSB lunar calibration. Currently, the lunar irradiance model developed by the United States Geological Survey (USGS) RObotic Lunar Observatory (ROLO) is widely used to correct the view geometry effect in the lunar calibration of most remote sensors [22], [23]. It has played an important role in the remote sensor calibration community over the last two decades. However, its uncertainty relative to the view geometry change becomes profound when higher accuracy is required for the calibration. In this analysis, it is shown that the uncertainty induces a seasonal oscillation in the RSB calibration coefficients derived from the scheduled lunar observations and even much larger oscillation in those derived from the unscheduled lunar observations due to much larger view geometry-related variations. It is demonstrated that the uncertainty of the ROLO model relative to view geometry in the lunar phase angle range covered by the MODIS lunar observations can be as large as 4%, which is much larger than the value of 1% as relative uncertainty for the entire phase angle range reported in [22]–[24] and the 2% calibration

accuracy requirement of many remote sensors [3], [4]. To improve the MODIS lunar calibration accuracy, a simple lunar model based on MODIS lunar observations in the time period from 2005 to 2012 is developed. With the model, the MODIS RSB lunar calibration results for the entire missions for both instruments, 2000–2020 for Terra MODIS and 2002–2020 for Aqua MODIS, are significantly improved. In this investigation, both the scheduled and unscheduled lunar observations are analyzed. It is shown that the unscheduled lunar observations can provide similar quality as the radiometric trending results for the MODIS RSB compared to the scheduled lunar views as long as the view geometry effect is accurately corrected.

The organization of this article is as follows. Section II briefly describes the lunar observations, lunar observation data, and oversampling effect. Section III reviews the MODIS RSB lunar irradiance formulism, shows the MODIS-measured lunar irradiances for both the scheduled and unscheduled MODIS lunar observations, and displays the strong effect of the view geometry, especially as a function of the lunar phase angle. Section IV reviews the MODIS RSB lunar calibration algorithm and shows the RSB lunar calibration results derived from both the scheduled and unscheduled lunar observations with view geometric effect corrected using ROLO model predictions. The seasonal oscillations and large uncertainties in the derived calibration coefficients, especially those from the unscheduled lunar observations, are demonstrated. In Section V, an analytical model for the lunar irradiance is developed and constructed based on the MODIS-measured lunar irradiance in the time period from 2005 to 2012. Section VI shows the improved RSB lunar calibration results for the entire missions for both the MODIS instruments by using the new lunar model for the view geometric effect correction. It is also shown that the calibration coefficients derived from the scheduled and unscheduled lunar observations are consistent and have a very good long-term agreement. Further improvements of the calibration coefficients are also discussed. Finally, conclusions and a summary are provided in Section VII.

II. MODIS LUNAR OBSERVATIONS

MODIS can view the Moon through both its EV port and its SV port. When it views the Moon through its EV port, a spacecraft pitch-over maneuver is required [6]. In this analysis, we concentrate on the lunar observations through the SV port. The view through the SV port forms a cone with a vertex of 7° as seen in Fig. 2. As MODIS circles in its orbit, the cone forms an annular ring, a hollow cone. The Moon is viewed whenever it passes through the annular ring. Without any spacecraft maneuver, both Terra MODIS and Aqua MODIS can view the Moon in three or four months every year through their SV port [19]–[21]. In each such occasion, the Moon is viewed in several continuous orbits by the instrument when it gets into the ring and also in several continuous orbits when it moves out of the ring. One set of the observations occur at the night side of Earth and the other at day side of Earth. There are more than 20 lunar observation events in each of the months for one instrument. In most

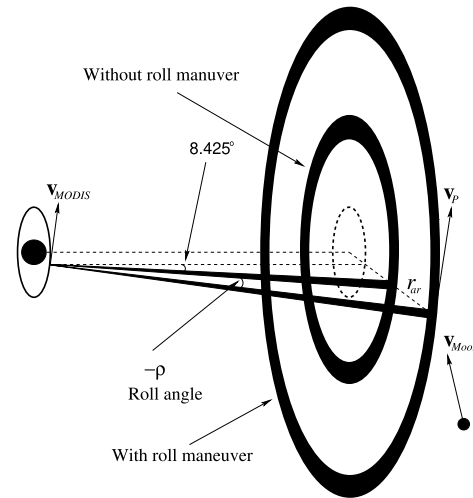


Fig. 2. Schematic for a lunar view with a roll maneuver. The roll angle is defined in the MODIS coordinate system and always has a negative value when the annular ring is enlarged.

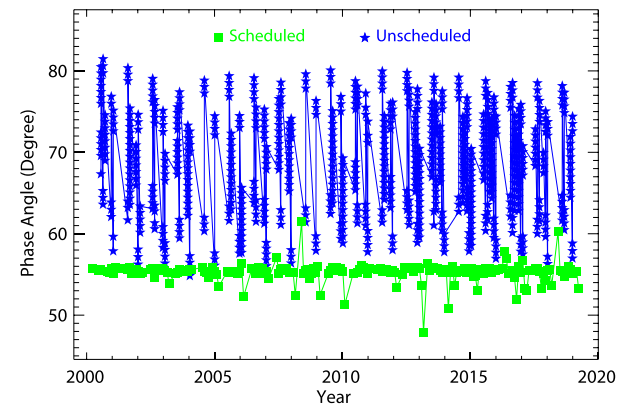


Fig. 3. Lunar phase angles of the Terra lunar observations.

of these lunar views, the Moon is only partially observed by MODIS. There are about 10 lunar views which fully cover the Moon, 5 at night side and 5 at day side of Earth. Every year there are about 30 such lunar observation events and only these lunar observations can be used to track the RSB on-orbit degradation as aforementioned.

The phase angles of these unscheduled MODIS lunar observations are randomly distributed over a large range from 55° to 82° for Terra MODIS and from -80° to -54° for Aqua MODIS, where a negative phase angle implies a waxing Moon. Terra MODIS and Aqua MODIS view a waning and waxing Moon due to their movement in a descending orbit and an ascending orbit, respectively. Fig. 3 shows the lunar phase angles for all Terra MODIS lunar observations. The blue stars are the lunar phase angles of the unscheduled lunar observations. It is demonstrated that the lunar phase angles of the observations in each month almost covers the entire range. It is known that the lunar irradiance strongly depends on lunar view geometry, especially the lunar phase angle. Thus, a key for the successful use of the unscheduled lunar observations to track the RSB on-orbit gain change is to correct the effect of the view geometry with high accuracy, which is the major challenge of this investigation.

A spacecraft roll maneuver can increase the chances of viewing the Moon and also provide the flexibility in the selection of the lunar phase angle for a lunar observation [5], [6]. Both Terra and Aqua are allowed to have a roll maneuver within roll angle in $[-20^\circ, 0^\circ]$ defined in MODIS coordinate system. Beyond the specified roll angle range, there is an instrument safety concern [5]. With a roll maneuver, both Terra MODIS and Aqua MODIS can be scheduled to view the Moon in about nine months every year. This at least doubles the number of months in which the Moon can be observed compared to the unscheduled lunar observations. The roll maneuver enables the selection of the lunar observations such that the lunar phase angles for the selected observations are confined within 1° [5], [6], which minimizes the accuracy requirement for the correction of the view geometry effect on the lunar irradiance. Thus, the lunar view with a roll maneuver is used for the MODIS instrument's routine lunar calibration. The lunar phases for the scheduled lunar views are confined in $[55^\circ, 56^\circ]$ for Terra MODIS and $[-56^\circ, -55^\circ]$ for Aqua MODIS. There are some occasions, in which the restriction is relaxed, due to various reasons as given in [5] and [6]. The green squares in Fig. 3 show the lunar phase angles for the scheduled lunar observations. The symbols a few degrees away from the straight green line are the cases where the restriction of the phase angle is relaxed, most likely caused by an observation within the phase angle restriction being unavailable for several months.

The orbits of Terra and Aqua were designed for viewing Earth so that the MODIS scan gap and overlap at nadir is nominally zero. However, when the MODIS views the Moon, there is considerable overlap of swaths on the lunar surface, which is called the oversampling effect. The overlap only occurs in the along-track direction [5] and its oversampling effect can be described by an oversampling factor, $f_{\text{os},B}$, which is the number of times the lunar surface is viewed by a detector of band B. The oversampling factor depends on the position of the sensor, the Moon–sensor distance, the velocities of the Moon and the sensor, as well as the roll angle of the maneuver [5]. It also depends on the spatial resolution of the band and, therefore, is band dependent. The oversampling factor can be calculated analytically according to the view geometry, roll angle, and the band number [5]. The roll angle for an unscheduled lunar observation is always set to be zero when the oversampling factor is calculated. Fig. 4 shows the oversampling factors for a 1-km band for all Terra MODIS lunar observations, where the blue stars are for the unscheduled lunar observations, while the green squares are for the scheduled lunar observations. The oversampling factor for an unscheduled lunar observation is usually larger than that for a scheduled lunar observation since the roll maneuver increases the speed of the MODIS view trajectory on the lunar surface [5]. For a 500- and 250-m band, the oversampling factors can be obtained from those displayed in Fig. 4 dividing by a factor of 2 and 4, respectively. For a lunar observation event, the entire lunar surface is evenly covered $f_{\text{os},B}$ times by every detector of the band if $f_{\text{os},B}$ happens to be an integer. However, in most cases, it is not an integer and then some part of the lunar surface is viewed by the times of

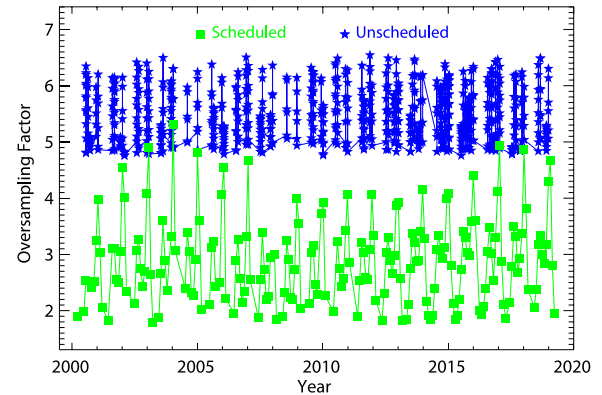


Fig. 4. Oversampling factors for the Terra lunar observations.

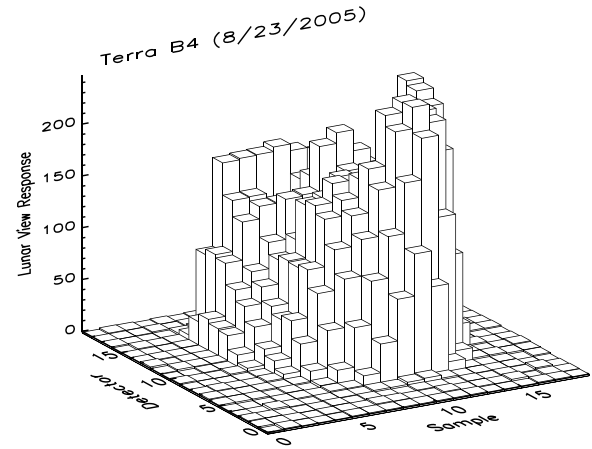


Fig. 5. Lunar image observed by all detectors of Terra MODIS band 4 in one scan on August 23, 2005.

the greatest integer less than the oversampling factor, while the remaining part is viewed one additional time by the detector [5]. Considering that there are ten detectors in a 1-km band, the oversampling factor of the whole band is $10f_{\text{os},B}$. In other words, it is those in Fig. 4 multiplying by a factor of 10. For each lunar observation event, the oversampling factor is exactly the same for all bands after including the factor to account for the spatial resolution differences for 500- and 250-m bands.

Due to the oversampling effect, the Moon is viewed in several scans in a lunar observation event, regardless of whether it is a scheduled or an unscheduled lunar observation. Because the Moon size is about 7×7 pixels of a 1-km band (such as MODIS band 8), the Moon can be fully covered by one MODIS scan. Fig. 5 depicts the background subtracted lunar view response of Terra MODIS band 4 on August 23, 2005, in one scan by all the 20 detectors of the band. Due to the oversampling effect, the lunar surface is viewed several times by the detectors of the band and then each detector of the band views the lunar surface multiple times during each lunar observation event. Fig. 6 shows a lunar image observed by Terra band 4 detector 5 on August 23, 2005, in multiple scans. The oversampling factor of band 5 for this lunar observation is 1.7 and thus, the lunar surface is viewed 1.7 times by the detector. An elongation effect is seen in the

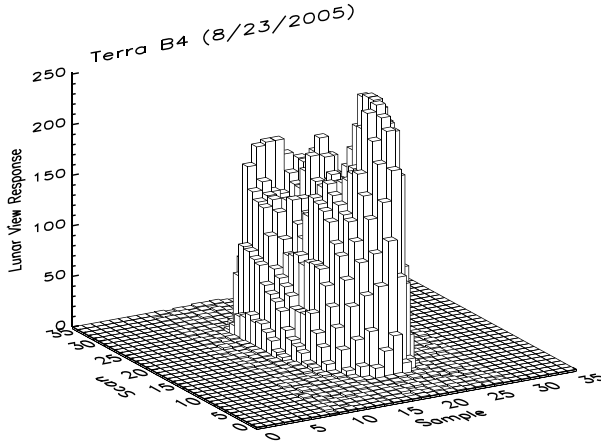


Fig. 6. Lunar image observed by one detector of Terra MODIS band 4 in multiple scans on August 23, 2005.

lunar image in Fig. 5 along the track direction due to fact that the oversampling factor is much larger than 1.

III. MODIS LUNAR IRRADIANCE

As listed in Table I, the MODIS RSB has three spatial resolutions at nadir: 250 m for bands 1–2, 500 m for bands 3–7, and 1 km for bands 8–19 and 26 [3], [4]. There are 40 detectors with 4 subframes, 20 detectors with 2 subframes, and 10 detectors for a 250-m, 500-m, and 1-km band, respectively. The MODIS lunar radiance is calculated in the same way as for the EV radiance [5]

$$L_{\text{Moon}}(B, D, S, F, N) = \frac{E_{\text{Sun}}(B, D)m_1(B, D, S, M_N)dn_{\text{Moon}}(B, D, S, F, N)}{\pi RVS(B, M, D, \alpha_{SV})} \quad (1)$$

where B , D , S , F , and N are band, detector, subframe, frame, and scan number, respectively, M_N is the mirror side (MS) of the N th scan, $E_{\text{Sun}}(B, D)$ is the MODIS relative spectral response (RSR) weighted solar irradiance, m_1 is the calibration coefficient, $dn_{\text{Moon}}(B, D, S, F, N)$ is the digital response corrected for background signal and the instrument temperature variations, RVS is the response versus scan angle, and α_{SV} is the AOI of the SV on the scan mirror.

As mentioned in Section II, each MODIS band can view the Moon in multiple scans due to the oversampling effect and there are scans in which the Moon is fully imaged by the band. The lunar irradiance can be calculated from the response of all detectors of the band in one or more scans. It can also be calculated from the response of one detector in multiple scans as long as the oversampling factor of the band is larger than 1. The third approach for the lunar irradiance calculation is to use the response of all detectors in multiple scans. The differences among the lunar irradiance derived from the three approaches are much smaller than the calibration uncertainty of the MODIS RSB and thus, one can use any of the three approaches to calculate the MODIS lunar irradiance and achieve equally meaningful results [5]. In the third approach, the MODIS lunar irradiance I_B for band B is

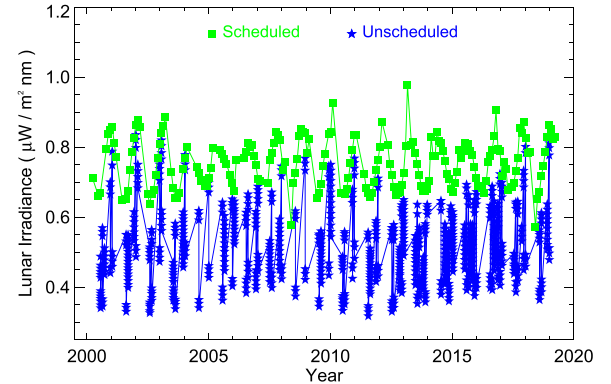


Fig. 7. Lunar irradiance measured by Terra MODIS band 8: squares, scheduled lunar observations and stars, unscheduled lunar observations.

calculated by [5]

$$I_B = \frac{1}{N_B f_{\text{os}, B}} \sum_{D, F, S, N} L_{\text{Moon}}(B, D, S, F, N) \omega_B \quad (2)$$

where N_B is the number of detectors in the band and ω_B is the solid angle (steradians) of each pixel of band B , which can be calculated from the pixel size of the band on Earth's surface at nadir and the height of the MODIS instrument. The pixel size along each direction can be easily calculated by $1/S_{\text{tot}}^B$, where S_{tot}^B is the number of subframes in one frame of the band B , which is 4, 2, and 1 for bands 1–2, 3–7, and others, respectively, as listed in Table I. The height of the MODIS on-orbit is known to be about 705 km above the Earth's surface. Then ω_B can be calculated by [5]

$$\omega_B = \frac{1}{(705 S_{\text{tot}}^B)^2}. \quad (3)$$

Both Terra MODIS Level 1B and Aqua MODIS Level 1B products have been reprocessed several times. Collection 6 (C6) of the L1B is the most recent version of the products for both instruments [28], [29]. Collection 6.1 is an improved version of the C6. For most RSBs, there are no difference between the products of L1B C6 and C6.1. In this analysis, the lunar irradiance is calculated for the RSB of the two instruments using the L1B C6.1 calibration coefficients. The measured lunar irradiance calculated from both the scheduled and unscheduled lunar observations for Terra MODIS band 8 and Aqua MODIS band 8 is shown in Figs. 7 and 8, respectively. The green squares represent the lunar irradiance from the scheduled lunar observations and the blue stars represent the unscheduled lunar views. As expected, the measured values of the lunar irradiance are strongly view geometry dependent, especially those for the unscheduled lunar observations whose phase angles are distributed over a larger phase angle range. For the scheduled lunar observations, the values of the lunar irradiance vary within 30%, while for the unscheduled lunar observations, the largest value of the lunar irradiance can be more than twice of the smallest one. This behavior is also observed in the lunar irradiance of other MODIS RSB.

As mentioned above, the green squares have a smaller magnitude of variations with time compared to the blue stars

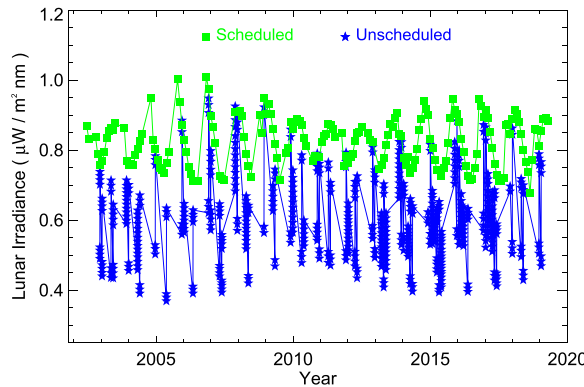


Fig. 8. Lunar irradiance measured by Aqua MODIS band 8: squares, scheduled lunar observations and stars, unscheduled lunar observations.

in both Figs. 7 and 8. This is due to the limit of the phase angle for the scheduled lunar observations in the small range from 55° to 56° for Terra MODIS and from -56° to -55° for Aqua MODIS in most cases. The variations seen in the lunar irradiance calculated from the scheduled lunar observations are mainly due to changes in the Sun–Moon distance, Moon–MODIS distance, and lunar librations [5]. The Sun–Moon distance varies about 3.35% in a period of one year, while the Moon–MODIS distance changes about 11.1% in a period of 29.5 days. Their impacts on the lunar irradiance are 6.7% and 22.2%. The effect of the lunar librations is relatively small, which is known to be about 2%. The variations seen in the lunar irradiance observed in the scheduled lunar observation are about 30% that is consistent with this estimate.

The unscheduled lunar observations occur only in three or four months every year for each MODIS instrument as mentioned earlier. In each of these months, the Moon is viewed in several continuous orbits when it gets into the annular ring formed by the view through the SV and also in several continuous orbits as it transitions in and out of the ring. The time difference between the two sets of orbits is less than two days. From Figs. 7 and 8, the lunar irradiance significantly changes among the lunar observations in each of the months. During the two-day time period, the instrument gain, the Sun–Earth distance, the Moon–MODIS distance, and even the lunar librations are known not to significantly change and thus, the large variation of the lunar irradiance shown in Figs. 7 and 8 among the unscheduled lunar observations is mainly due to the phase angle variations.

The dependence of the lunar irradiance on the Sun–Earth distance and that on the Moon–MODIS distance can be described analytically and, thus, can be easily removed. Figs. 9 and 10 show the measured lunar irradiance with the effect of the Sun–Earth and Moon–MODIS distance being corrected for Terra MODIS band 8 and Aqua MODIS band 8, respectively. The variations of the lunar irradiance now are due to the change of the lunar phase angle and the lunar libration angles. Since the lunar phase angles are confined to a 1° range for the scheduled lunar observations, while those for the unscheduled lunar observations are spread out over a large range, the fluctuations among the symbols of the green squares in Figs. 9 and 10 are much smaller than those

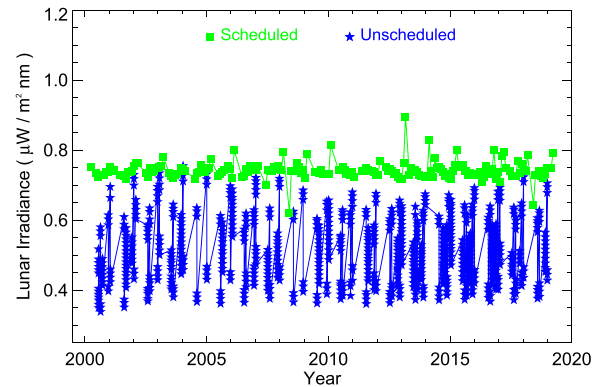


Fig. 9. Lunar irradiance measured by Terra MODIS band 8 and corrected with the Sun–Moon distance and Moon–sensor distance effect: squares, scheduled lunar observations and stars, unscheduled lunar observations.

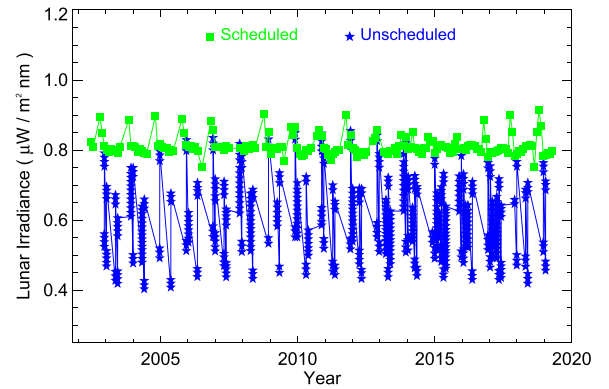


Fig. 10. Lunar irradiance measured by Aqua MODIS band 8 and corrected with the Sun–Moon distance and Moon–sensor distance effect: squares, scheduled lunar observations and stars, unscheduled lunar observations.

among the symbols of blue stars. However, there are some undulations in the scheduled lunar observations (shown in green squares) in both Figs. 9 and 10. As mentioned previously and as demonstrated in Fig. 3, there are some exceptions in the scheduled lunar observations for which the confinement of phase angle is relaxed due to various reasons [5]. Comparing Figs. 3 and 9, one can easily correlate the peaks and valleys in Fig. 9 to the outliers in the phase angles of the scheduled lunar observations in Fig. 3. From the two plots, one can also see the correlation between the lunar irradiance and phase angles. Similarly, the out-of-family-scheduled lunar measurements in Fig. 10 are due to the relaxation of the phase angle confinement. For the data shown in Figs. 9 and 10 for band 8 and also those for other RSB, the lunar phase curve and the dependence of the lunar irradiance on the lunar librations can be derived at the wavelengths of the MODIS RSB in the phase angle range covered by the unscheduled lunar observations for both waxing Moon and waning Moon.

IV. MODIS LUNAR CALIBRATION COEFFICIENTS

The lunar surface has a very stable reflectance in the visible and near-infrared spectral regions [24]. Therefore, the lunar surface can be used as light source to characterize the on-orbit degradation of the MODIS RSB. Different from SD, the lunar surface is not a smooth target. With a known lunar irradiance and the measured lunar irradiance based on (2), it is

possible to calculate the calibration coefficients for MODIS by forcing them to be equal. It is critical to know the lunar irradiance for the view geometry of a lunar observation if the calibration coefficients of the RSB are to be derived from the lunar observation. Intensive investigations have been performed in the last several decades to simulate and predict the lunar irradiance and its dependence with view geometry and wavelength of the observing channel [24]–[27]. So far, the ROLO lunar model developed by Kieffer and Stone [27] is the most widely used model for simulating the lunar irradiance in the remote sensor calibration community. It is still very challenging to accurately predict the lunar irradiance for a lunar observation event, especially the absolute value of the irradiance. Thus, lunar calibration is mainly used to track the instrument's on-orbit degradation [5], [11]–[13].

To track the instrument's on-orbit degradation instead of absolute calibration, only relative dependence of the lunar irradiance with respect to the view geometry is needed. In principle, the calibration coefficients can be derived for each band, detector, MS, and subframe. Since different detectors and subframes may observe slight different parts of the Moon and as the lunar surface is not smooth, the calibration coefficients for individual detector and subframe may have larger uncertainty. In this investigation, we focus on the detector- and subframe-averaged calibration coefficients, which are required in the derivation of time-dependent RVS [7]. The detector- and subframe-averaged lunar coefficient for band B and MS M can then be calculated by [5], (4) as shown at the bottom of the page, where $f_{vg,B}$ describes the dependence of the lunar irradiance on the view geometry, $E_{Sun}(B,D)$ is the MODIS RSR weighted solar irradiance, and $m_1^0(B, D, S, M)$ is the first on-orbit measured calibration coefficient derived from the SD/SDSM calibration [3], [4]. The view geometry factor $f_{vg,B}$ can be obtained from the results of the ROLO lunar model. However, the ROLO model may not be very accurate to describe the dependence of the lunar libration angles nor the lunar phase angle dependence over a large range. The former induces annual oscillation in the derived calibration coefficients, while the latter impacts the unscheduled lunar observations where the lunar phase angles are observed to cover a wide range. In the later sections, this issue will be addressed in more detail and a lunar model based on MODIS measurements will be developed to improve the MODIS RSB lunar calibration. The inverse of the lunar calibration coefficient, $1/m_1^{Moon}(B, M)$, tracks the gain change of MODIS electronic and optical systems since the first lunar measurement for band B and MS M at the AOI of the SV.

The detector- and subframe-averaged calibration coefficients for the RSB of the two MODIS instruments have been derived from both the scheduled and unscheduled lunar observations using (4). In the calculation, the ROLO lunar model results are used as $f_{vg,B}$ to account for the view geometry variations. For the scheduled lunar observations, the background sub-

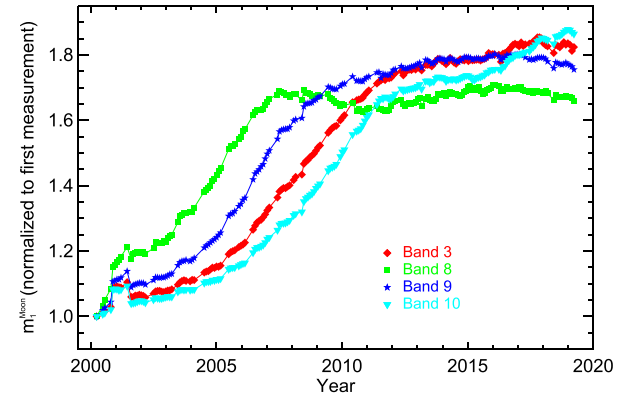


Fig. 11. Lunar calibration coefficients derived from the scheduled lunar observations for Terra MODIS bands 3, 8, 9, and 10 MS1.

tracted instrument response dn_{Moon} is obtained from the L1A data of the EV sector, while for the unscheduled lunar observations, the instrument responses are taken from the data of the SV sector. A sector rotation is applied to move the SV data to EV sector during every scheduled lunar observation, while no sector rotation is applied for any unscheduled lunar observation.

The detector- and subframe-averaged calibration coefficients derived from the scheduled lunar observations for Terra MODIS bands 3, 8, 9, and 10 MS 1 are displayed in Fig. 11. They are normalized to the first measurement for each band. The coefficients are stable and change with time smoothly except around day 305 on-orbit (October 31, 2000) and day 549 (July 2, 2001). The discontinuities around the two days in the coefficients are due to switches of the MODIS electronics from side A to the redundant sideband from side B back to side A. Early in the mission, the coefficients of all four bands increase with time and the bands with shorter wavelength increase faster than the bands with longer wavelength. Since the calibration coefficients are inversely proportional to the gain of the band, all four bands degrade with time and the band with short wavelength experiencing faster degradation. In the first seven years, the coefficients of band 8 increased about 70%, corresponding to a gain degradation of 41%, and then reached its maximum value. In the next three years, the coefficients decrease a few percent and then keep almost constant in the following years. As mentioned earlier, bands 9, 3, and 10 degrade slower than band 8 during early mission but they degrade faster later and their degradation surpassed that of band 8 in 2009, 2010, and 2011, respectively. The four curves of the coefficients all become flat after 2011. This means that the bands were stable in the last eight years. Band 3 slightly degrades over the last two years, while band 10 degrades much faster, a cumulative of 3% since 2017. After 19 years on-orbit, bands 3, 8, 9, and 10 degrade about 45%, 42%, 44%, and 46%, respectively. This indicates that among these four bands, the band with longer wavelength degrades more in

$$m_1^{Moon}(B, M) = \frac{\pi N_B f_{os,B} f_{vg,B}}{\sum_{D,F,S,N} E_{Sun}(B, D) m_1^0(B, D, S, M) dn_{Moon}(B, D, F, S, N)} \quad (4)$$

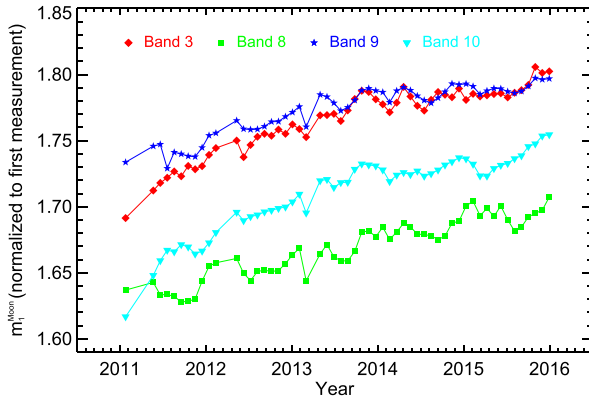


Fig. 12. Same lunar calibration coefficients as those in Fig. 11 but only for the time period from 2011 to 2016.

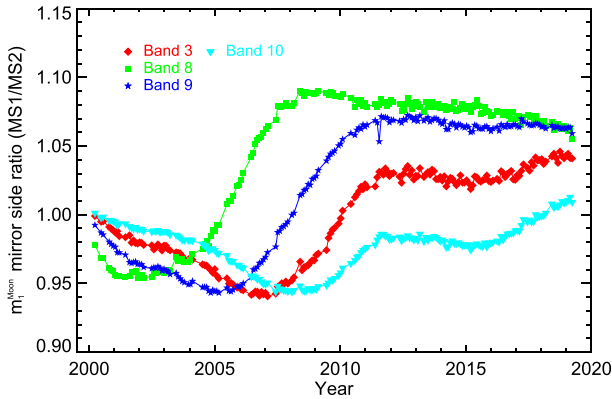


Fig. 13. Lunar calibration coefficients MS ratio derived from the scheduled lunar observations for Terra MODIS bands 3, 8, 9, and 10.

the long term, which is opposite to the pattern of wavelength dependence of the degradation early in the mission.

It is worth drawing attention to the oscillations that are seen in Fig. 11. To highlight them more clearly, the calibration coefficients for the time period from 2011 to 2016 are redrawn in Fig. 12. It can be seen from Fig. 12 that the amplitudes of the oscillations are greater than 1%. It is definitely desirable to eliminate or reduce the oscillations considering the calibration specification of the MODIS RSBs is 2%. This issue will be discussed more in Section VI.

Fig. 13 shows the MS ratio of the lunar calibration coefficients for Terra MODIS bands 3, 8, 9, and 10. From Fig. 13, it can be seen that MS2 of the scan mirror degrades faster than MS1 for the four bands in early mission. This means that the calibration coefficients of the four bands for MS2 increase faster than those for MS1 as shown in Fig. 11. After five years on-orbit, the MS2 at the wavelength of band 8 (412 nm) started to degrade at a slower rate than MS1. The MS ratio for band 8 increases about 15% in a very short time period around 2006. The same as band 8, bands 3, 9, and 10 MS2 degrade faster early in mission and then became slower than MS1 in 2010, 2008, and 2019, respectively. The MS ratios of the calibration coefficients for the four bands became flat after they reach their first maxima at slightly different times. The ratios for bands 3 and 10 started to increase again over the last two

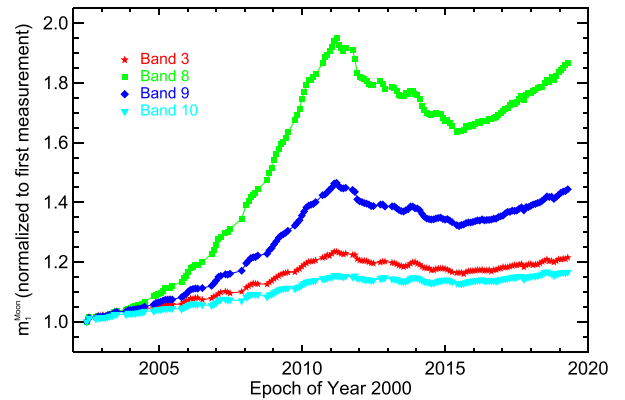


Fig. 14. Lunar calibration coefficients derived from the scheduled lunar observations for Aqua MODIS bands 3, 8, 9, and 10 MS1.

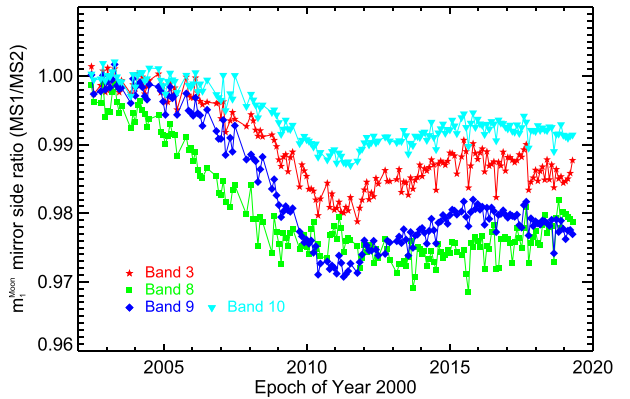


Fig. 15. Lunar calibration coefficients MS ratio derived from the scheduled lunar observations for Aqua MODIS bands 3, 8, 9, and 10.

years. The large variations of the MS ratios of the calibration coefficients demonstrate that the degradation of the reflectance of the Terra MODIS scan mirror is very different for the two MSs.

Fig. 14 shows similar plots for Aqua MODIS bands 3, 8, 9, and 10 MS1. Similar to Terra MODIS RSB, the derived lunar calibration coefficients are stable and smooth. In the first nine years on-orbit, the coefficients for all four bands increase steadily with time at a larger degradation rate at short wavelengths. They reach their maxima all at the same time around the beginning of 2011, after which they show a decrease until the middle of 2015 and once again increase over the last four years. The decrease in the magnitude of the calibration coefficients indicates that the gains of the bands increased in the time period contrary to the expected decreasing trend. The exact reason behind this abnormal behavior is not fully understood yet. By comparing MS1 calibration coefficients in Figs. 11 and 14, it can be seen that the four short-wavelength bands of the two instruments perform very differently. Fig. 15 shows the MS ratios of the calibration coefficients for Aqua MODIS bands 3, 8, 9, and 10, which look noisier compared to those of Terra MODIS in Fig. 13 due to the much smaller scale of the y-axis. The ratios for the four bands first all decreased with time, then reached their local minima around the beginning of 2011, started to increase with

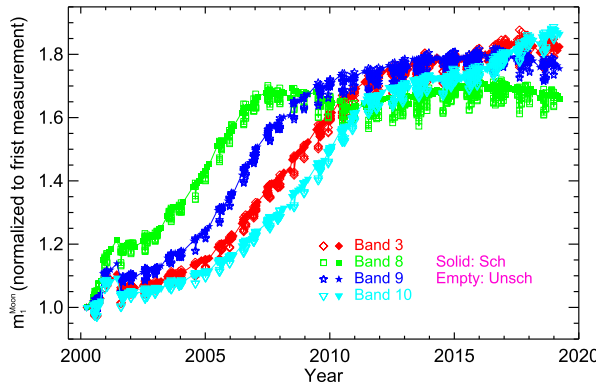


Fig. 16. Lunar calibration coefficients derived from both the unscheduled and scheduled lunar observations for Terra MODIS bands 3, 8–10, and 18 scan MS one.

time after the minima, arrived their local maxima around the middle of 2015, and finally decreased with time again in the last four years. The MS ratios for bands 3, 8, 9, and 10 are all within 2%, 3%, 3%, and 1%, respectively. Compared to Terra MODIS, the Aqua MS differences are much smaller.

The calibration coefficients for bands 1, 2, 4, 11, 12, 17, 18, and 19 for both instruments are derived from the scheduled lunar observations as well. The results are stable and smooth as expected. The calibration coefficients including those for bands 3, 8, 9, and 10 are used to routinely generate the RSB calibration look up tables (LUTs), especially the time-dependent RVS of the scan mirrors for MODIS L1B products [5], [7]. For bands 13–16, they saturate during a lunar observation and because of this, it is hard to get accurate calibration coefficients from the lunar observations. The short-wave infrared (SWIR) bands 5–7 and 26 are contaminated by the crosstalk contaminations among themselves and those from middle wave infrared (MWIR) bands 20–25. To get reliable calibration coefficients for the SWIR bands, the crosstalk contamination need to be removed, which is beyond the scope of this article. In this article, we focus on bands 1–4, 8–12, and 17–19.

Fig. 16 shows the detector- and subframe-averaged lunar calibration coefficients derived from both the scheduled and unscheduled lunar observations for Terra MODIS bands 3, 8, 9, and 10 MS1. In Fig. 16, solid symbols denote those from the scheduled lunar observations, while empty symbols denote the unscheduled observations. From Fig. 16, the two sets of coefficients match reasonably well with one another. However, when they are checked carefully, it can be clearly seen that the coefficients derived from the unscheduled lunar observations occur in the same month spread out in a range of several percent, 4% or more for band 8. Since the instrument does not change much in a time period of a few days, the variation of the 4% is likely from the uncertainty of the view geometry effect correction. Also, due to the fact that the lunar librations do not change much in such a short period of time, the uncertainty of the 4% should be mainly due to the ROLO model with respect to the lunar phase angle in a large range of 27° from 55° to 82° as shown in Fig. 3.

Fig. 17 shows the detector- and subframe-averaged lunar calibration coefficients derived from both the scheduled and

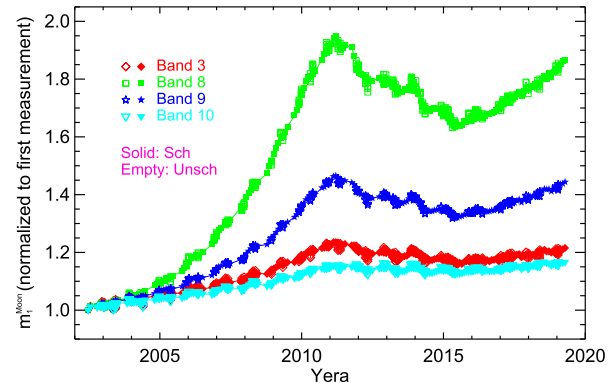


Fig. 17. Lunar calibration coefficients derived from both the unscheduled and scheduled lunar observations for Aqua MODIS bands 3, 8–10, and 18 scan MS one.

unscheduled lunar observations for Aqua MODIS bands 3, 8, 9, and 10 MS1. As is shown for Terra RSB, the two sets of the calibration coefficients derived from the scheduled (solid symbols) and unscheduled (empty symbols) lunar observations match each other quite well. In fact, the differences between them are smaller than those observed in the Terra MODIS RSB lunar calibration coefficients. Nevertheless, the divergence between the coefficients is easily seen in Fig. 17. From Fig. 17, it can be seen that the magnitude of the divergence is about 2%. This further confirms the necessity of the improvement of the ROLO model for prediction of the view geometry effect on the lunar irradiance.

The variation of the 4% observed in the lunar calibration coefficients indicates that the ROLO model needs to be further improved when it is applied to MODIS unscheduled lunar observations, where the lunar phase angles vary over a range of about 27° . This also means that one should be very careful when an intercomparison between two remote sensors is performed using the Moon as reference and the ROLO model results as the bridge for the view geometry effect [17], [18] as the relative uncertainty of the ROLO model with respect to view geometry can be as large as 4%. By carefully examining Figs. 11 and 14, one can also find that the uncertainties in the calibration coefficients derived from the scheduled lunar observations are 1% or larger, even though the phase angles are limited within a small range of 1° . Since the phase angles are limited in a small range, the errors should mainly come from the uncertainty of the view geometry effect correction with respect to the lunar librations. Thus, the ROLO model results also have an uncertainty of about 1% with respect to the lunar librations. This 1% uncertainty of the ROLO lunar model with respect to the lunar librations has also been found in the lunar calibration of other sensors when the ROLO model is used to correct the view geometric effect [10]–[13]. Thus, the improvement of the ROLO lunar model with respect to description of both the lunar phase angle and the lunar libration effect on the lunar irradiance is necessary.

V. LUNAR MODEL-BASED MODIS OBSERVATIONS

As mentioned previously, the ROLO lunar model has played a very critical role in the last two decades for the lunar calibration of the remote sensors, especially in MODIS,

SeaWiFS, and VIIRS RSB on-orbit calibration [5], [10]–[13]. However, the model was developed based on ground measurements [24], [26], [27], which may have a large uncertainty in the absolute lunar irradiance due to various reasons. To date, lunar calibration is mainly used to track the on-orbit change of a remote sensor because of the large absolute uncertainty associated with the model. The relative uncertainty of the model with respect to view geometry variation is known to be smaller than the absolute uncertainty [22]–[24]. It could still be larger than expected for lunar calibration of instruments with high accuracy requirements, especially when the lunar phase angle spans a large range.

Significant effort has been devoted to improve the ROLO lunar model by S. Wagner *et al.* and Global Space-based Intercalibration System (GSICS) lunar calibration working group [30]. In this investigation, the lunar irradiance measured by Terra MODIS and Aqua MODIS, both the scheduled and unscheduled lunar observations, are used to derive a simple yet accurate lunar model for the lunar irradiance for the phase angle range covered by the MODIS lunar observations. The absolute uncertainty of this model will be the same as that of the MODIS RSB calibration. The relative uncertainty of the model with respect to the view geometry will be greatly improved since the observation geometry of a lunar observation should have no impact on the uncertainty of the MODIS-measured lunar irradiance.

The lunar irradiance can be expressed as

$$\gamma I(\lambda, \phi, \alpha, \beta, \gamma, r_{\text{SM}}, r_{\text{MS}}) = \frac{\Theta(\lambda, \phi)[1 + L(\lambda, \phi, \alpha, \beta, \gamma)]}{r_{\text{SM}}^2 r_{\text{MS}}^2} \quad (5)$$

where λ is the wavelength of the Sunlight reflected by the Moon, ϕ is the lunar phase angle, α is the lunar longitude libration angle from the view of the sensor, β is the lunar latitude libration angle from the view of the sensor, γ is the lunar latitude libration angle from view of the Sun, r_{SM} is the Sun–Moon distance in astronomical unit (AU), and r_{MS} is the Moon–sensor distance normalized by its mean value. $\Theta(\lambda, \phi)$ describes the dependence of the irradiance on the lunar phase angle which is called the lunar phase curve and $L(\lambda, \phi, \alpha, \beta, \gamma)$ describes the effect of the lunar librations. Compared to $\Theta(\lambda, \phi)$, $L(\lambda, \phi, \alpha, \beta, \gamma)$ is a small quantity and changes within about $\pm 3\%$ with respect to the lunar longitude and latitude librations, both of which vary within the range from -9° to 9° , and lunar latitude libration from the view of the Sun which varies from -1.5° to 1.5° . Then a quadratic approximation with respect to α and β and a linear approximation with respect to γ can be used to describe the effect of the lunar librations, e.g.,

$$L(\lambda, \phi, \alpha, \beta, \gamma) = c_1(\lambda, \phi)\alpha + c_2(\lambda, \phi)\beta + c_3(\lambda, \phi)\alpha^2 + c_4(\lambda, \phi)\beta^2 + \gamma c_5(\lambda, \phi)\alpha\beta + c_6\lambda \quad (6)$$

where c_1, \dots, c_5 are coefficients of the quadratic approximation for α and β and c_6 is the coefficient for the linear approximation for γ . $L(\lambda, \phi, \alpha, \beta, \gamma)$ accounts for the change in the lunar irradiance with respect to the libration angles relative to the case where all three libration angles are zero.

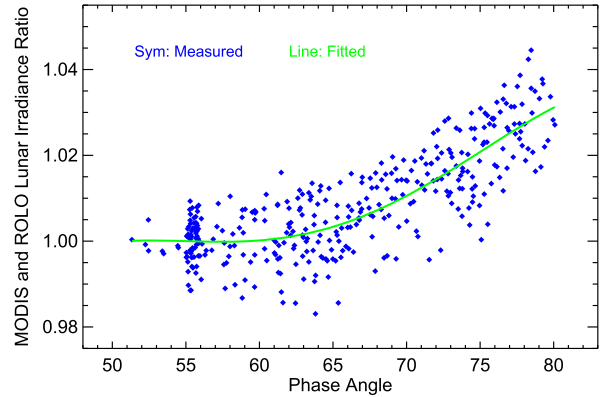


Fig. 18. MODIS and ROLO model lunar irradiance ratios at the wavelength of MODIS band 8. The ratios are normalized at the phase angle of 55° .

The aforementioned angles play an important role in the exact measurement of the lunar brightness as viewed by the sensor. The first two angles α and β are the libration angles in terms of longitude and latitude, which define the azimuth and elevation angles with respect to the Earth's coordinate system. The variations of these two angles are restricted to within $\pm 9^\circ$. On the other hand, the lunar libration angle γ created by the slow variation of the solar elevation angle and varying within $\pm 1.5^\circ$. However, it will be shown in the subsequent paragraphs that the impact of this angle will contribute to about 1% in the overall Lunar brightness measurement. By mitigating the angles mentioned in (6), the overall Lunar irradiance would be well captured and be a considerable improvement over the current ROLO model.

The phase curve, $\Theta(\lambda, \phi)$, at a given wavelength can be expressed as a polynomial of the phase angle ϕ . For MODIS lunar observations, the lunar phase angles span a range from 48° to 82° , as shown in Fig. 3, for a waning Moon and from -81° to -50° for a waxing Moon. The former is covered by Terra MODIS, while the latter is done by Aqua MODIS. For each of the lunar phase angle ranges, a fourth-order polynomial of the phase angle can be used to describe the phase curve for each of the wavelengths of the MODIS RSB, i.e.,

$$\phi \Theta(\lambda, \phi) = a_0(\lambda) + a_1(\lambda)\phi + a_2(\lambda)\phi^2 + a_3(\lambda)\phi^3 + a_4(\lambda)\phi^4 \quad (7)$$

where a_0 , a_1 , a_2 , a_3 , and a_4 are the coefficients of the polynomial.

Before moving further to fit the MODIS lunar irradiance to (6) and (7), it would be better to examine the differences between the MODIS-measured and ROLO-model-predicted lunar irradiance. Fig. 18 shows the ratios (blue squares) of the lunar irradiance measured by Terra MODIS band 8 and the ROLO-model-predicted lunar irradiance at the wavelength of MODIS band 8. To minimize the impact of the MODIS calibration uncertainties, only the data in the time period from the beginning of 2005 to the end of 2012 are used in the plot. As mentioned previously, the MODIS lunar irradiance is calculated using MODIS L1B C6.1. MODIS L1B C6 for both instruments started in operation in 2012 and thus, the reprocessed and refined calibration coefficients were used for the L1B products before 2012, while those after 2012 were

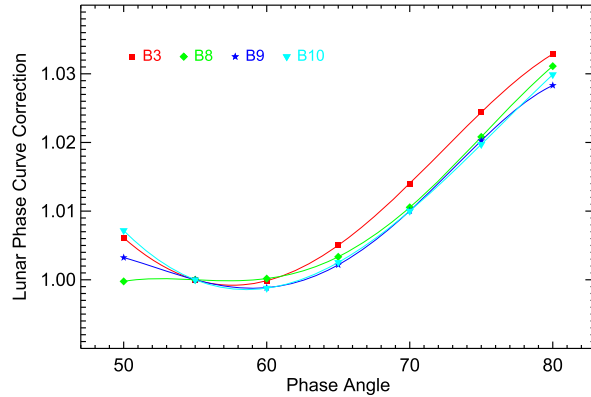


Fig. 19. MODIS and ROLO model lunar irradiance ratios at wavelengths of bands 3, 8, 9, and 10.

generated with forward LUTs for the calibration coefficients. Thus, the latter may have relatively larger uncertainty than the former. The L1B products may have a relatively larger uncertainty as well early in each mission due to various instrument adjustments and tests. Due to the aforementioned concerns, only the data in the time period from the beginning of 2005 to the end of 2012 are used for the ratios of the two sets of the lunar irradiance. As shown in Fig. 18, there is sufficient data in the time period for this analysis. It can be clearly seen from the blue squares in the plot that ratios vary with the lunar phase angles. The measured ratios are fitted to a fourth-order polynomial described in (7) and the green solid line is the fitted polynomial. The fluctuations of the measured ratios are due to the uncertainty of the description of the ROLO model with respect to lunar librations. The instrument calibration uncertainty and other factors may have contributions to the fluctuations as well. Since the lunar calibration is used to track the MODIS RSB orbit changes, only the variation of the lunar irradiance with respect to view geometry is needed. Thus, the ratios and the fitted curve in Fig. 18 are normalized to the fitted curve at phase angle 55°. The value of the fitted curve at 55° before the normalization is 1.0534, which means that the lunar irradiance measured by Terra MODIS band 8 at the phase angle of 55° is about 5.34% higher than that predicted by the ROLO model for that wavelength and phase angle. From the fitted curve, it can be seen that the ROLO model may have a relative uncertainty of 3.2% with respect to the lunar phase angle range from 48° to 80° besides the aforementioned uncertainty of 5.34% at phase angle of 55°, which is much larger than the estimated relative uncertainty reported in [24], [26], [27].

Similar to Terra band 8, the ratios of Terra MODIS-measured and ROLO-model-predicted lunar irradiance at the wavelengths of other RSB can be calculated and fitted to the polynomial in (7). Fig. 19 shows the fitted curves for Terra MODIS bands 3, 8, 9, and 10. The curves are normalized at the phase angle of 55°. It is clearly visible that the four fitted curves are very close to each other. This means that the relative uncertainties at the wavelengths of bands 3, 9, and 10 with respect to the lunar phase angle in the range from 50° to 80° are all about 3%, which is about the same as that at the wavelength of band 8. The relative uncertainties of the

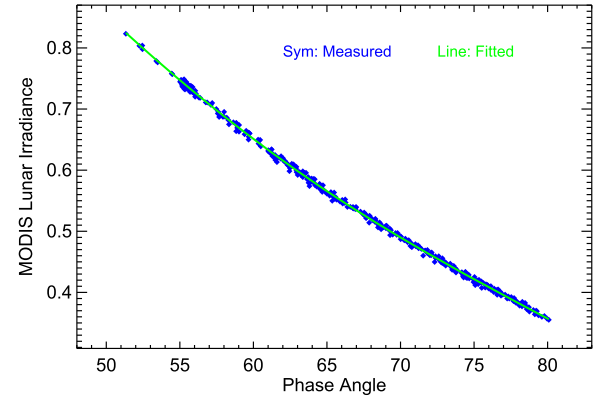


Fig. 20. MODIS lunar irradiance observed by Terra band 8. The Sun–Earth distance and Moon–MODIS distance effects on the radiance have been removed. The effect of the lunar librations has been removed as well using the ROLO-model-predicted values for the effect.

ROLO model in the aforementioned phase angle range at wavelengths of other MODIS RSB are close to 3% as well. Similar to Terra MODIS, the ratios of Aqua MODIS-measured and ROLO-model-predicted lunar irradiance can be calculated and fitted to the fourth-order polynomial. According to the fitted curves, the relative uncertainties of the ROLO model with respect to the lunar phase angle in the angle range from -80° to -50° are about 2% or less at the wavelengths of the MODIS RSB. This indicates that relative uncertainties of the ROLO model are smaller for a waxing Moon than those for a waning Moon. Nevertheless, a relative uncertainty of 2% is still much larger than the estimated relative uncertainty reported in [24], [26], [27] and definitely makes the calibration uncertainty larger than the specification for the remote sensors like MODIS and VIIRS which have a 2% calibration specification for the RSBs considering there are other significant contributions to the instrument calibration uncertainty.

The lunar irradiance measured by Terra band 8 via the lunar phase angle are displayed in Fig. 20 as blue squares. With the same rationale as mentioned previously, only data in the time period from the beginning of 2005 to the end of 2012 are shown in the plot. The effects of the Sun–Earth distance and Moon–MODIS distance on the lunar irradiance are removed and the effect of the lunar librations is also corrected by using the predictions of the ROLO model for the effect. Thus, the measured lunar irradiance shown by the blue squares, displayed in Fig. 20, represent the lunar irradiance of a waning Moon at the wavelength of MODIS band 8 in the phase angle range from 51° to 80°. These measured irradiances are fitted to the fourth-order polynomial described in (7) and the green curve is the fitted polynomial. It is clearly seen that the fitted polynomial and the measured values match very well in the entire phase angle range. This indicates that the fourth-order polynomial can describe the lunar phase curve in the phase angle range accurately. The fitting residuals vary within $\pm 1\%$ and are partially due to the uncertainty of the lunar libration effect correction provided by the ROLO model and partially due to the uncertainty of the MODIS L1B C6.1. This effect will be further delved upon in the subsequent paragraphs.

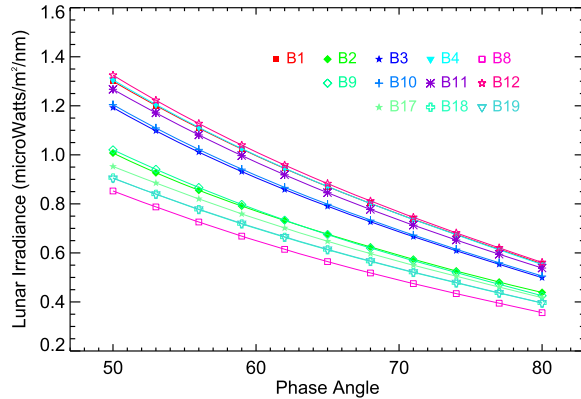


Fig. 21. Lunar phase curves derived from the Terra MODIS lunar observations for a waning Moon at wavelengths of the MODIS RSB.

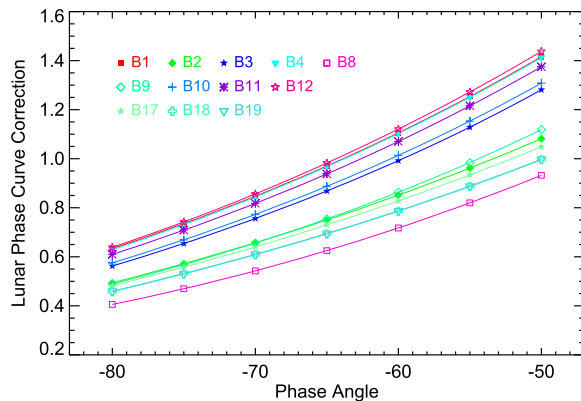


Fig. 22. Lunar phase curves derived from the Aqua MODIS lunar observations for a waxing Moon at wavelengths of the MODIS RSB.

With the same procedure as used above, the measured lunar irradiance by other Terra MODIS RSB is fitted to the fourth-order polynomial and the lunar phase curves for a waning Moon at the wavelengths of the RSB are derived. Fig. 21 shows the obtained lunar curves for the wavelengths of MODIS bands 1–4, 8–12, and 17–19 in the phase angle range from 50° to 80°. The lunar phase curves are strongly wavelength dependent and decrease dramatically with phase angle as expected. Similarly, the lunar phase curves for a waxing Moon at the wavelengths of the MODIS RSB can be derived from the lunar irradiance measured by Aqua MODIS RSB. Fig. 22 shows the derived lunar phase curves for the phase angle range from –80° to –50° at the wavelengths of MODIS bands 1–4, 8–12, and 17–19. By comparing Figs. 21 and 22, it can be seen that the lunar phase curves for a waning and waxing Moon for the same wavelength via absolute phase angle are about the same as expected. However, with careful examination, it can be seen that a lunar phase curve for a waxing Moon is always higher than that for a waning Moon for the same wavelength. The fitted coefficients of the polynomials, a_0 – a_4 , for all the derived lunar phase curves are listed in Table II. With these coefficients, one can easily calculate the phase curves derived from the MODIS lunar observations.

As previously discussed, the lunar irradiance corrected for the Sun–Earth and the Moon–MODIS distance are given

TABLE II
MODIS LUNAR PHASE CURVE COEFFICIENTS

	Band	a_0	a_1	a_2	a_3	a_4
Terra	1	2.5738329	0.0231296	-0.0021426	3.01E-05	-1.40E-07
	2	6.7587307	-0.2795609	0.0052386	-4.72E-05	1.60E-07
	3	4.7703432	-0.1242709	0.0013438	-5.88E-06	0.00E+00
	4	4.0542127	-0.0662204	-0.0000827	8.91E-06	-5.00E-08
	8	1.5048679	0.0253840	-0.0015669	2.03E-05	-9.00E-08
	9	2.4695824	-0.0071936	-0.0011039	1.75E-05	-8.00E-08
	10	4.5533491	-0.1109170	0.0010704	-3.59E-06	0.00E+00
	11	3.7055596	-0.0564533	-0.0000997	7.12E-06	-4.00E-08
	12	4.9317458	-0.1207815	0.0012239	-5.05E-06	0.00E+00
	17	1.0332402	0.0622821	-0.0024246	2.89E-05	-1.20E-07
	18	2.2008510	-0.0133998	-0.0006970	1.17E-05	-6.00E-08
	19	1.3183889	0.0387380	-0.0018463	2.30E-05	-1.00E-07
	1	3.3406120	0.0305918	-0.0005117	-9.04E-06	-4.00E-08
	2	2.5636394	0.0271802	-0.0002539	-5.28E-06	-2.00E-08
	3	5.0937049	0.1525857	0.0023500	1.99E-05	7.00E-08
	4	3.5172804	0.0426878	-0.0002154	-5.91E-06	-3.00E-08
	8	2.1516974	0.0138413	-0.0005200	-7.73E-06	-3.00E-08
	9	4.0491352	0.1076295	0.0014529	1.14E-05	4.00E-08
	10	4.4201605	0.1074147	0.0012858	9.06E-06	3.00E-08
	11	3.9746933	0.0744874	0.0005307	1.70E-06	0.00E+00
	12	4.2969245	0.0888982	0.0008600	5.36E-06	2.00E-08
	17	3.2086873	0.0738807	0.0009062	7.09E-06	2.00E-08
	18	2.1704829	0.0135215	-0.0004986	-7.62E-06	-3.00E-08
	19	3.4953449	0.0971588	0.0014652	1.27E-05	5.00E-08

in Figs. 9 and 10, respectively. The residual effects as seen in Figs. 9 and 10 can be further dissected and accounted for using the derived lunar phase curves. The ratios mainly bear the information of the lunar libration effect even though they may also include the relative errors of the RSB calibration and those due to other sources. The absolute errors of the RSB calibration should be already included in the lunar phase curves. As expressed in (6) and mentioned previously, the lunar libration effect on the lunar irradiance should depend on the lunar phase and the three lunar libration angles, α , β , and γ . As demonstrated in Fig. 3, the lunar phase angles of the Terra lunar observations are distributed uniformly varying from 50° to 80° except at the small subrange from 55° to 56°, where there are many more observations due to the scheduled Terra lunar observations. Similarly, the lunar phase angles of Aqua lunar observations are almost evenly distributed in the phase angle range from –80° to –50° with exception in a narrow range of –56° to –55° due to the contributions of the scheduled lunar observations.

There are a total of 363 Terra MODIS lunar observations in the time period from the beginning of 2005 to the end of 2012. For the available lunar acquisitions, the phase angle range from 50° to 80° can be divided into four subranges, [50°, 56°], [56°, 64.5°], [64.5°, 72.5°], and [72.5°, 80°], and then the calculated ratios can be separated into four groups. For each of the subgroups, there are about or more than 70 lunar observations. The averaged values of the phase angles in the four subranges are 55°, 61°, 68°, and 76°. The four phase angles are the corner stone and will be used to calculate the effect of the lunar librations $L(\lambda, \varphi, \alpha, \beta, \gamma)$ described in (6). Fig. 23 shows the derived $L(\lambda, \varphi, \alpha, \beta, \gamma)$ for a waning Moon with respect to lunar libration angles α and β at $\lambda = 412$ nm, with $\varphi = 55^\circ$ and $\gamma = 0^\circ$. It can be easily seen that the effect changes

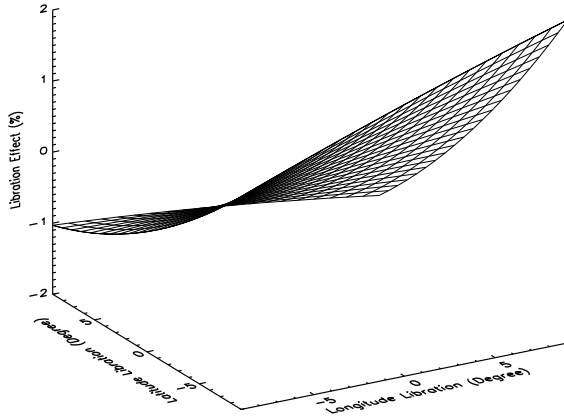


Fig. 23. $L(412 \text{ nm}, 55^\circ, \alpha, \beta, 0^\circ)$ derived from the lunar irradiance measured by Terra MODIS band 8.

within $\pm 2\%$. The lunar irradiance simply decreases with latitude libration angle β but has a more complex relationship with longitude libration angle α . It increases with longitude libration angle when latitude libration angle is negative, while it may decrease when the latitude libration angle becomes positive. The derived functions of $L(\lambda, \varphi, \alpha, \beta, \gamma)$ at the other three phase angles for the wavelength of MODIS band 8 confirm that $L(\lambda, \varphi, \alpha, \beta, \gamma)$ is indeed phase angle dependent and the dependence is not negligible considering the lunar calibration accuracy requirements of the remote sensors. The effects of the lunar irradiance with respect to lunar libration angles α and β at wavelengths of other MODIS RSB are derived as well. From them, it can be confirmed that they are wavelength dependent as expected.

The same procedure is applied to derive $L(\lambda, \varphi, \alpha, \beta, \gamma)$ for a waxing Moon using Aqua MODIS lunar observations. There are a total of 290 Aqua MODIS lunar observations in the time period from the beginning of 2005 till the end of 2012. The phase angle range varying from -80° to -50° can be divided into four subranges $[-80^\circ, 72.5^\circ]$, $[-70^\circ, -64.5^\circ]$, $[-64.5^\circ, 56^\circ]$, and $[-56^\circ, -50^\circ]$. For each subdivision, there are about 60 Aqua lunar observations. Similar to Terra MODIS, the averaged values of the phase angles in the four groups are -74° , -67° , -61° , and -55° . Then by following exactly the same procedure applied to Terra MODIS, the effects of the lunar librations $L(\lambda, \varphi, \alpha, \beta, \gamma)$ for a waxing Moon at all four phase angles for each of the wavelengths of MODIS bands 1–4, 8–12, and 17–19 are derived from the Aqua MODIS lunar observations. Fig. 24 shows the derived $L(\lambda, \varphi, \alpha, \beta, \gamma)$ for a waxing Moon with respect to lunar libration angles α and β at $\lambda = 412 \text{ nm}$, $\varphi = -55^\circ$ and $\gamma = 0^\circ$. Comparing Figs. 23 and 24, it can be easily seen that the effect of the librations, α and β , on the lunar irradiance is obviously larger for a waxing Moon than for a waning Moon and the relationships of the effects for the two phases of the Moon are apparently different, especially with respect to latitude libration angle β . The close dependence of the libration effect on the wavelength and the phase is confirmed from the derived functions as well.

As expressed in (6), the effect of the lunar librations not only depends on the lunar libration angles α and β

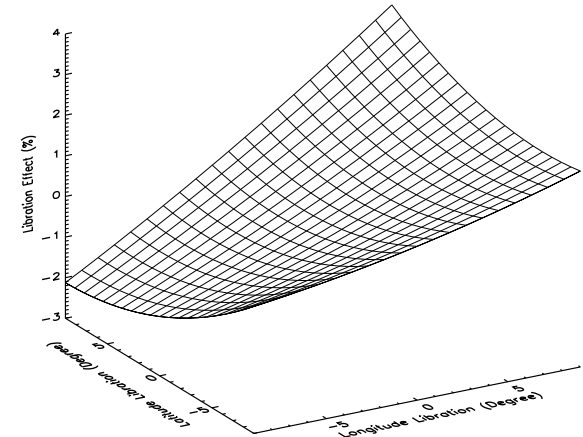


Fig. 24. $L(412 \text{ nm}, -55^\circ, \alpha, \beta, 0^\circ)$ derived from the lunar irradiance measured by Aqua MODIS band 8.

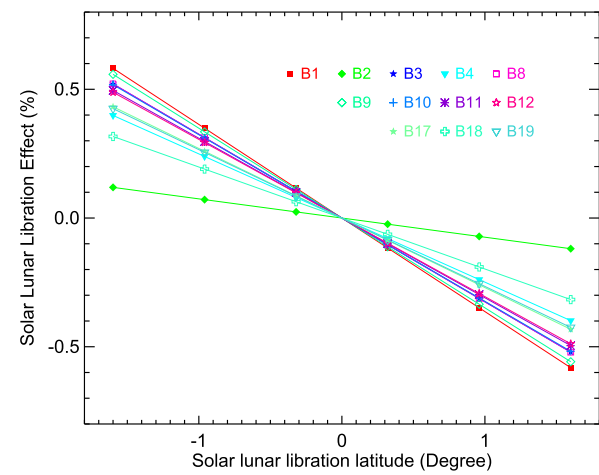


Fig. 25. $L(\lambda, 55^\circ, 0^\circ, 0^\circ, \gamma)$ derived from the lunar measurements of Terra MODIS for a waxing Moon at phase angle 55°.

(from the view of the remote sensor) but also on the libration angle γ (from the view of the Sun). Fig. 25 shows the effect of lunar librations with respect to γ for a waxing Moon at phase angle of 55° for the wavelengths of MODIS bands 1–4, 8–12, and 17–19 derived from the Terra MODIS lunar observations. The effects are clearly wavelength dependent and the impacts on the lunar irradiance can be as large as 1.2% for most of the bands, which can induce seasonal oscillations with the amplitudes of 1.2% in the derived lunar calibration coefficients. This is a direct effect due to the libration angle γ . Comparing the effect of the librations with respect to α and β , it is smaller by a factor of 4 but definitely needs to be removed in order to achieve highly accurate calibration coefficients from the lunar observations even if only the scheduled lunar observations are considered. The functions $L(\lambda, \varphi, 0^\circ, 0^\circ, \gamma)$ at the other three phase angles are very close to those displayed in Fig. 25. Fig. 26 shows the effect of lunar libration with respect to γ for a waxing Moon at the phase angle of -55° for the wavelengths of MODIS bands 1–4, 8–12, and 17–19 derived from the Aqua MODIS lunar observations. The effects are much smaller than those in a waning Moon but still can induce seasonal oscillations with the amplitudes of 0.5% in the

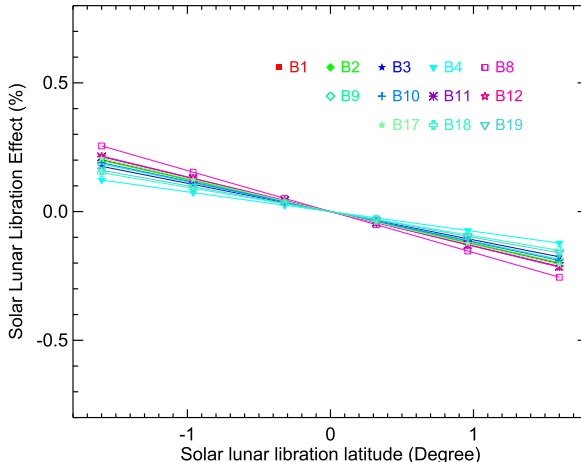


Fig. 26. $L(\lambda, -55^\circ, 0^\circ, 0^\circ, \gamma)$ derived from the lunar measurements of Aqua MODIS for a waxing Moon at phase angle -55° .

derived Aqua RSB lunar calibration coefficients if the effects are ignored in Aqua lunar calibration.

The fitted coefficients c_1 – c_6 of the libration effects, $L(\lambda, \varphi, \alpha, \beta, \gamma)$, at phase angle 55° for a waning Moon and at -55° for a waxing Moon are listed in Table III. The coefficients for the libration effects at the other three phase angles for either a waning or a waxing Moon are also derived from the MODIS lunar observations. The lunar libration effect at any other phase angle φ in the phase angle range either $[-80^\circ, -50^\circ]$ or $[50^\circ, 80^\circ]$ can be obtained by a linear interpolation of the two functions, $L(\lambda, \varphi_1, \alpha, \beta, \gamma)$ and $L(\lambda, \varphi_2, \alpha, \beta, \gamma)$, where $\varphi_1 < \varphi < \varphi_2$.

With the derived lunar phase curves, $\Theta(\lambda, \varphi)$, and the effect of lunar librations, $L(\lambda, \varphi, \alpha, \beta, \lambda)$, it is possible to construct a lunar model which covers the lunar phase angle range varying from -80° to -50° and from 50° to 80° . The absolute uncertainty of the model is about the same as that of the MODIS RSB calibration and the relative uncertainty with respect to the view geometry is the relative uncertainty of the MODIS RSB geolocation, which should be much smaller than the total uncertainty of the MODIS instruments since the uncertainty of the MODIS measurements does not depend on lunar view geometry, while the view geometry is determined with high accuracy. The model can be applied to MODIS lunar calibration for both the scheduled and unscheduled lunar observations. Further, this model can also be applied to other remote sensors for their lunar characterization as well.

It is worth emphasizing that the lunar model described in this article is derived using the MODIS-measured lunar irradiance only in the time period from the beginning of 2005 to the end of 2012 as aforementioned. The model only covers two pieces of the phase range, -80° to -50° and 50° to 80° . The model for the first piece of phase angle is derived from Aqua lunar measurements, while for the second piece, it is derived from the Terra lunar observations. For the application of the new model to the RSB lunar calibration of a remote sensor, whether the model for the first piece or the second one should be applied depends on whether a waxing Moon or a waning Moon is viewed by the sensor. The model can only provide the

TABLE III
COEFFICIENTS FOR LUNAR LIBRATION EFFECT
AT AN ABSOLUTE PHASE ANGLE OF 55°

	Band	c_1	c_2	c_3	c_4	c_5	c_6
Terra	1	0.000101	-0.001295	3.51E-05	8.50E-05	-9.06E-06	-0.003634
	2	-0.000149	-0.002224	5.92E-05	3.03E-05	1.62E-05	-0.000744
	3	0.000241	-0.001590	3.35E-05	5.90E-05	-1.92E-05	-0.003254
	4	0.000167	-0.001547	3.57E-05	5.97E-05	-3.44E-05	-0.002491
	8	0.000287	-0.001698	-6.32E-06	3.61E-05	-6.37E-05	-0.003256
	9	0.000293	-0.001623	1.60E-05	5.25E-05	-3.30E-05	-0.003488
	10	0.000230	-0.001623	3.27E-05	5.20E-05	-4.00E-05	-0.003235
	11	0.000095	-0.001540	5.24E-05	5.03E-05	-3.16E-05	-0.003098
	12	0.000139	-0.001518	4.99E-05	4.49E-05	-3.10E-05	-0.003053
	17	0.000118	-0.001711	4.86E-05	5.19E-05	-2.46E-05	-0.002702
	18	0.000005	-0.001860	6.91E-05	3.38E-05	-2.02E-05	-0.001980
	19	0.000110	-0.001749	6.31E-05	4.08E-05	-3.20E-05	-0.002656
Aqua	1	0.001865	-0.000414	1.73E-05	8.80E-05	2.52E-05	-0.001259
	2	0.002033	-0.000405	3.46E-06	6.83E-05	3.44E-05	-0.001242
	3	0.001812	-0.000410	-4.30E-06	8.55E-05	6.32E-05	-0.001098
	4	0.001831	-0.000530	1.40E-05	6.03E-05	3.08E-05	-0.000765
	8	0.001917	-0.000274	2.30E-05	6.64E-05	1.08E-04	-0.001594
	9	0.001868	-0.000395	-6.23E-06	8.60E-05	8.45E-05	-0.001157
	10	0.001878	-0.000464	7.10E-07	8.41E-05	4.54E-05	-0.001187
	11	0.001897	-0.000398	2.10E-05	7.25E-05	4.29E-05	-0.001331
	12	0.001861	-0.000361	1.70E-05	7.05E-05	4.75E-05	-0.001348
	17	0.002217	-0.000359	6.46E-06	7.40E-05	5.70E-05	-0.001289
	18	0.002259	-0.000394	5.70E-06	6.49E-05	5.68E-05	-0.000943
	19	0.002292	-0.000415	6.91E-06	6.37E-05	5.69E-05	-0.001003

lunar irradiance at 12 discrete wavelengths in spectral range from 412 to 940 nm. However, for any wavelength in the aforementioned range, a linear interpolation can be applied to get the model results from those at the 12 wavelengths.

In Section VI, the model will be applied to both the Terra and Aqua lunar calibrations for the entire mission, from 2000 to 2020 for Terra MODIS and from 2002 to 2020 for Aqua MODIS. This will be a direct validation of the construction of the model in this section and also a critical step of the assessment of the model on the application in the RSB lunar calibration of a remote sensor. Further assessment of the model may need the application of the model to the lunar calibration of other remote sensors, which will be future work and is beyond the scope of this article.

VI. IMPROVEMENTS IN THE MODIS LUNAR CALIBRATION COEFFICIENTS

The lunar irradiance model developed in Section V based on MODIS lunar measurements in the time period from 2005 to 2012 can be applied back to improve the accuracy in MODIS lunar calibration. The lunar calibration coefficients have been recalculated using the scheduled and unscheduled lunar observations for the entire mission for both instruments, 2000 to 2020 for Terra MODIS and 2002 to 2020 for Aqua MODIS. Also, corrected are the view angle dependencies as discussed earlier.

Fig. 27 shows the lunar calibration coefficients of Terra MODIS bands 3, 8, 9, and 10 from the scheduled lunar observations with the view geometric effect corrected by the new lunar model. Compared with those in Fig. 11, it can be seen that the newly derived coefficients are more stable and vary in a smooth fashion. There are clear oscillations seen in the

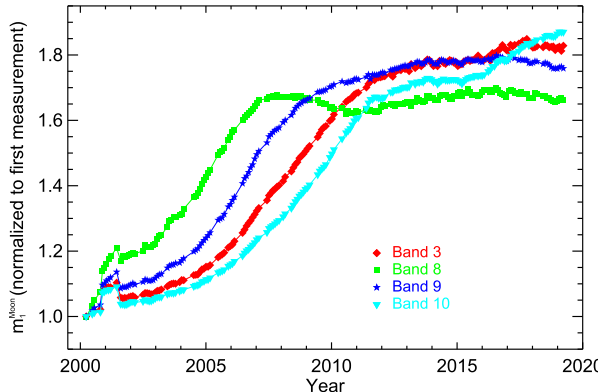


Fig. 27. Lunar calibration coefficients derived from the scheduled lunar observations for Terra MODIS bands 3, 8, 9, and 10 MS1.

calibration coefficients displayed in Fig. 11 and these oscillations become considerably stronger later in mission. By using the predictions of the newly developed lunar irradiance model to correct the view geometric effect in (4), the oscillations are significantly reduced, especially early in mission. In other words, the calibration coefficients are remarkably improved. Nevertheless, one can find that there are still some residual oscillations in late mission and amplitudes of the oscillations are larger in the bands with shorter wavelengths, especially in band 8. Since the oscillations only remain late in late mission, they should not be induced by the errors of the lunar irradiance model. They must be caused by some other mechanisms which need to be further investigated. However, based on the rich calibration experience of MODIS, in particular the short-wavelength bands as shown in Fig. 27, it is plausible that these residual oscillations are induced due to the polarization effect. Previous works reported in [31]–[33] have identified calibration errors induced by polarization that has a direct impact on the oscillations seen in the m_1 coefficient, it has been reported that sensitivities due to polarization were minimal in the first 8 years of the mission time for Terra MODIS. Thereafter, the polarization had reached as high as 8% for band 8 and became as high as 30% in 2011. Similar trends were observed for the remaining bands (3, 9, and 10). However, the intensities were quite small and their high points were slightly different as polarization is extremely wavelength dependent. These effects were clearly captured by the oscillations seen in the long-term m_1 and RVS trends. Hence, the residual oscillations seen in the aforementioned lunar trends are likely due to the Moonlight polarization effect. Further analysis on this effect is undergoing and will be reported elsewhere.

Fig. 28 shows the lunar calibration coefficients of Aqua MODIS bands 3, 8, 9, and 10 from the scheduled lunar observations with the view geometric effect corrected by our new lunar model. The same as for the Terra MODIS RSB, the newly derived calibration coefficients are more stable and smoother than those shown in Fig. 13. This demonstrates again that the newly developed lunar irradiance model can provide better prediction for the view geometric effect on the lunar irradiance for the application in the MODIS lunar calibration. Different from the Terra lunar calibration coefficients shown in Fig. 27, there are no clear seasonal oscillations being

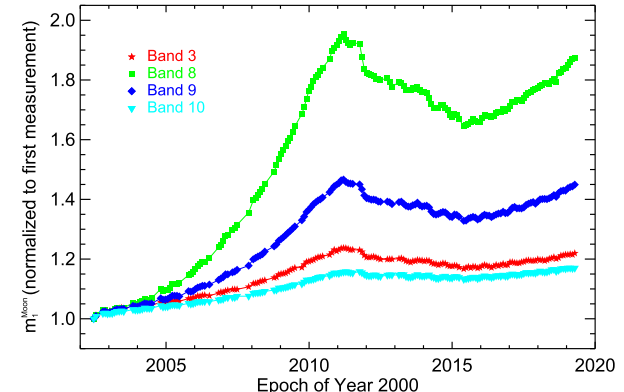


Fig. 28. Lunar calibration coefficients derived from the scheduled lunar observations for Aqua MODIS bands 3, 8, 9, and 10 MS1.

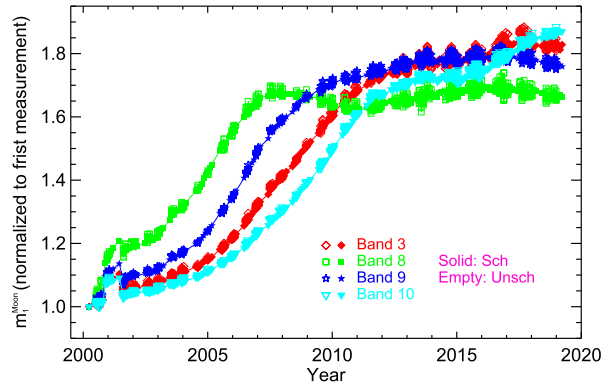


Fig. 29. Lunar calibration coefficients derived from both the unscheduled and scheduled lunar observations for Terra MODIS bands 3, 8, 9, and 10 MS1.

found in the recalculated Aqua lunar calibration coefficients. For both the Terra and Aqua scheduled lunar observations, the lunar phase angles are restricted in small ranges and the uncertainties of view geometric effect corrections are mainly due to the description errors of the lunar irradiance model with respect to the lunar librations. Thus, the improvements of the lunar calibration coefficients in Figs. 27 and 28 over those in Figs. 11 and 13 are mainly due to the improvements of our new lunar irradiance model over the ROLO lunar model in the effect of lunar librations. In fact, the seasonal oscillations in the derived lunar calibration coefficients due to the inadequate description of the libration effect in the ROLO model have been reported in [10]–[12]. However, whether the new model improves the lunar calibration results over the ROLO model for other sensors is unknown even though it is expected. The assessment of the new model's performance in the lunar calibration of other sensors is beyond the scope of this article.

Fig. 29 shows the lunar calibration coefficients for Terra MODIS bands 3, 8, 9, and 10 derived from both the scheduled and unscheduled lunar observations. Compared to those in Fig. 16, it is seen that the recalculated coefficients using the new lunar irradiance model for the view geometric effect correction are much improved, especially early in mission. The improvements are mainly due to the improvements of the lunar phase curves in the new lunar irradiance model compared to the ROLO model for MODIS lunar calibration application. Again there remain seasonal oscillations in the

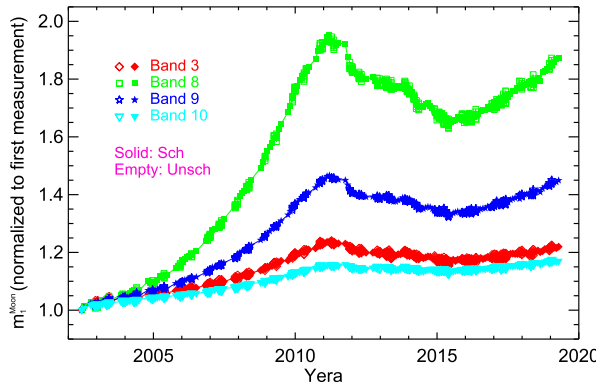


Fig. 30. Lunar calibration coefficients derived from both the unscheduled and scheduled lunar observations for Aqua MODIS bands 3, 8, 9, and 10 MS1.

calibration coefficients as shown in Fig. 29; however, they are greatly improved when compared to the coefficients shown in Figs. 11 and 12. As mentioned earlier, the oscillations are remarkably enhanced, especially late in mission, and amplitudes of the oscillations are found to be wavelength dependent. As discussed previously, the remaining seasonal oscillations should not be induced by the errors of the lunar irradiance model. They must be caused by some other mechanisms and is highly speculative that the Moonlight polarization could be the root cause. Fig. 30 shows the lunar calibration coefficients for Aqua MODIS bands 3, 8, 9, and 10 derived from both the scheduled and unscheduled lunar observations. The same as those for the Terra MODIS RSB, the recalculated coefficients using the new lunar irradiance model for the view geometric effect correction are significantly improved compared to those displayed in Fig. 17 and the improvements are mainly due to the improvements of the lunar phase curves in the new lunar irradiance model over those in the ROLO model for MODIS lunar calibration application. Compared to those in Fig. 28, it is easy to see that the calibration coefficients derived from the unscheduled lunar observations have larger uncertainties, appearing as small oscillations, the amplitudes of which are wavelength dependent.

It is well demonstrated in this section that new lunar model developed based on MODIS lunar observations in the time period from 2005 to 2012 significantly improves the MODIS lunar calibration results for the entire missions compared to the current ROLO model and will be applied in MODIS routine RSB lunar calibration using the scheduled lunar observations. Nevertheless, there are still visible seasonal oscillations in the improved calibration coefficients late in mission, especially in those derived from the unscheduled lunar observations, and the amplitudes of the oscillations are larger in the bands with shorter wavelengths. It has been mentioned previously that the oscillations may not be induced by the uncertainty of the lunar irradiance model but other mechanisms such as the polarization effect of the Moonlight. Further investigation on this issue is ongoing and will be discussed in the future.

VII. CONCLUSION

Both the scheduled and unscheduled lunar observations of the two MODIS instruments are analyzed even though

only the scheduled lunar observations are currently used to provide calibration coefficients for MODIS operational L1B products. Both the lunar irradiance at the wavelengths of the MODIS RSB and the calibration coefficients of the RSB are calculated for the entire mission for the two MODIS instruments. The measured lunar irradiance strongly depends on the view geometry and the wavelength. It is demonstrated that the calibration coefficients derived from the unscheduled lunar observations have larger uncertainties, which are about 4% for the Terra MODIS RSB. It is identified that the large uncertainties are mainly due to the uncertainties of the ROLO lunar model, which is used to correct the lunar view geometric effect in the current MODIS lunar calibration. Based on the MODIS lunar irradiance measured in the time period from 2005 to 2012, a new lunar irradiance model is developed for the phase angle range varying from 50° to 80° (a waning Moon) and -80° to -50° (a waxing Moon). The new model has been applied to recalculate the calibration coefficients for both the scheduled and unscheduled lunar observations and for the entire mission for both Terra MODIS and Aqua MODIS. It is clearly demonstrated that the new lunar irradiance model significantly improves the MODIS lunar calibration results for both the scheduled and unscheduled lunar observations. The lunar irradiance model developed in this investigation will be applied for the MODIS RSB routine lunar calibration using the scheduled lunar observations in near future. It can be applied to the lunar calibrations in other remote sensors as well. Visible oscillations are still observed in the calibration coefficients even though they are reduced after the new lunar irradiance model is applied. The oscillations may not be induced by the uncertainty of the lunar irradiance model but some other mechanisms such as moonlight polarization effect which will be further investigated.

ACKNOWLEDGMENT

The authors would like to thank Tom Stone for providing ROBOTIC LUNAR OBSERVATORY (ROLO) lunar model results and helpful information. They would also like to thank Sriharsha Madhavan, Daniel O. Link, and Amit Angal, for their helpful comments and suggestions. The views, opinions, and findings contained in this article are those of the authors and should not be construed as an official NASA or U.S. Government position, policy, or decision.

REFERENCES

- [1] W. L. Barnes and V. V. Salomonson, "MODIS: A global imaging spectroradiometer for the Earth observing system," *Crit. Rev. Opt. Sci. Technol.*, vol. CR47, pp. 285–307, 1993.
- [2] B. Guenther *et al.*, "MODIS calibration: A brief review of the strategy for the at-launch calibration approach," *J. Atmos. Ocean. Technol.*, vol. 13, no. 2, pp. 274–285, Apr. 1996.
- [3] X. Xiong *et al.*, "Multiyear on-orbit calibration and performance of Terra MODIS reflective solar bands," *IEEE Trans. Geosci. Remote Sens.*, vol. 45, no. 4, pp. 879–889, Apr. 2007.
- [4] X. Xiong, J. Sun, X. Xie, W. L. Barnes, and V. V. Salomonson, "On-orbit calibration and performance of Aqua MODIS reflective solar bands," *IEEE Trans. Geosci. Remote Sens.*, vol. 48, no. 1, pp. 535–545, Jan. 2010.
- [5] J. Sun, X. Xiong, W. L. Barnes, and B. Guenther, "MODIS reflective solar bands on-orbit lunar calibration," *IEEE Trans. Geosci. Remote Sens.*, vol. 45, no. 7, pp. 2383–2393, Jul. 2007.

- [6] J. Sun and X. Xiong, "Solar and lunar observation planning for Earth-observing sensor," *Proc. SPIE*, vol. 8176, Oct. 2011, Art. no. 817610.
- [7] J. Sun, X. Xiong, A. Angal, H. Chen, A. Wu, and X. Geng, "Time-dependent response versus scan angle for MODIS reflective solar bands," *IEEE Trans. Geosci. Remote Sens.*, vol. 52, no. 6, pp. 3159–3174, Jun. 2014.
- [8] J. Sun, M. Chu, and M. Wang, "Degradation nonuniformity in the solar diffuser bidirectional reflectance distribution function," *Appl. Opt.*, vol. 55, no. 22, pp. 6001–6016, 2016.
- [9] J. L. Roujean, M. J. Leroy, and P. Y. Deschamps, "A bidirectional reflectance model of the Earth's surface for the correction of remote sensing data," *J. Geophys. Res.*, vol. 97, no. D18, pp. 20455–20468, Dec. 1992.
- [10] J. Sun, X. Xiong, and J. Butler, "NPP VIIRS on-orbit calibration and characterization using the Moon," *Proc. SPIE*, vol. 8510, Oct. 2012, Art. no. 851011.
- [11] X. Xiong, J. Sun, J. Fulbright, Z. Wang, and J. J. Butler, "Lunar calibration and performance for S-NPP VIIRS reflective solar bands," *IEEE Trans. Geosci. Remote Sens.*, vol. 54, no. 2, pp. 1052–1061, Feb. 2016.
- [12] J. Sun and M. Wang, "NOAA-20 VIIRS on-orbit calibration and characterization using the Moon," *Proc. SPIE*, vol. 10764, Sep. 2018, Art. no. 107640U.
- [13] R. A. Barnes, R. E. Eplee, Jr., F. S. Patt, and C. R. McClain, "Changes in the radiometric sensitivity of SeaWiFS determined from lunar and solar-based measurements," *Appl. Opt.*, vol. 38, no. 21, pp. 4649–4664, 1999.
- [14] X. Xiong, J. Sun, S. Xiong, and W. L. Barnes, "Using the Moon for MODIS on-orbit spatial characterization," *Proc. SPIE*, vol. 5234, pp. 480–487, Feb. 2004.
- [15] J. Sun, X. Xiong, S. Madhavan, and B. N. Wenny, "Terra MODIS band 27 electronic crosstalk effect and its removal," *IEEE Trans. Geosci. Remote Sens.*, vol. 52, no. 3, pp. 1551–1561, Mar. 2014.
- [16] W. Li, X. Xiong, K. Chiang, and G. Toller, "Evaluation of Terra MODIS PC bands optical leak correction algorithm," *Proc. SPIE*, vol. 5882, Aug. 2005, Art. no. 588219.
- [17] X. Xiong, J. Sun, and W. Barnes, "Intercomparison of on-orbit calibration consistency between Terra and Aqua MODIS reflective solar bands using the Moon," *IEEE Geosci. Remote Sens. Lett.*, vol. 5, no. 4, pp. 778–782, Oct. 2008.
- [18] R. E. Eplee, Jr., J.-Q. Sun, G. Meister, F. S. Patt, X. Xiong, and C. R. McClain, "Cross calibration of SeaWiFS and MODIS using on-orbit observations of the Moon," *Appl. Opt.*, vol. 50, no. 2, pp. 120–133, 2011.
- [19] A. Angal, X. Xiong, and T. Wilson, "Intercomparison of Terra and Aqua MODIS using unscheduled lunar observations," *Proc. SPIE*, vol. 10785, Sep. 2018, Art. no. 107851T.
- [20] J. Sun, X. Xiong, and W. Barnes, "MODIS reflective solar bands unscheduled lunar observations," *Proc. SPIE*, vol. 6677, Oct. 2007, Art. no. 66771K.
- [21] T. Wilson, A. Angal, and X. Xiong, "Sensor performance assessment for terra and aqua MODIS using unscheduled lunar observations," *Proc. SPIE*, vol. 10785, Sep. 2018, Art. no. 1078519.
- [22] T. C. Stone, H. H. Kieffer, and K. J. Becker, "Modeling the radiance of the Moon for on-orbit calibration," *Proc. SPIE*, vol. 5151, pp. 463–470, Nov. 2003.
- [23] T. C. Stone and H. H. Kieffer, "Use of the Moon to support on-orbit sensor calibration for climate change measurements," *Proc. SPIE*, vol. 6296, pp. 62960Y-1–62960Y-9, Sep. 2006.
- [24] H. H. Kieffer, "Photometric stability of the lunar surface," *Icarus*, vol. 130, no. 2, pp. 323–327, Dec. 1997.
- [25] A. P. Lane and W. M. Irvine, "Monochromatic phase curves and albedos for the lunar disk," *Astron. J.*, vol. 78, pp. 267–277, Apr. 1973.
- [26] H. H. Kieffer and R. L. Wildey, "Establishing the Moon as a spectral radiance standard," *J. Atmos. Oce. Technol.*, 13, no. 2, pp. 360–375, 1996.
- [27] H. H. Kieffer and T. C. Stone, "The spectral irradiance of the Moon," *Astronomical J.*, vol. 129, no. 6, pp. 2887–2901, Jun. 2005.
- [28] J. Sun *et al.*, "MODIS reflective solar bands calibration improvements in collection 6," *Proc. SPIE*, vol. 8528, Nov. 2012, Art. no. 85280N.
- [29] G. Toller *et al.*, "Terra and aqua moderate-resolution imaging spectroradiometer collection 6 level 1B algorithm," *J. Appl. Remote Sens.*, vol. 7, no. 1, May 2013, Art. no. 073557.
- [30] S. Wagner, X. Hu, S. Wang, T. Stone, X. Wu, X. Xiong, and T. Hewison, "Outcomes of the second joint GSICS-CEOS/IVOS lunar calibration workshop," *GSICS Quart.*, vol. 11, no. 3, 2017, doi: [10.7289/V5833Q81](https://doi.org/10.7289/V5833Q81).
- [31] J. Sun and X. Xiong, "MODIS polarization-sensitivity analysis," *IEEE Trans. Geosci. Remote Sens.*, vol. 45, no. 9, pp. 2875–2885, Sep. 2007.
- [32] G. Meister, E. J. Kwiatkowska, B. A. Franz, F. S. Patt, G. C. Feldman, and C. R. McClain, "Moderate-resolution imaging spectroradiometer ocean color polarization correction," *Appl. Opt.*, vol. 44, no. 26, p. 5524, Sep. 2005.
- [33] E. J. Kwiatkowska, B. A. Franz, G. Meister, C. R. McClain, and X. Xiong, "Cross calibration of ocean-color bands from moderate resolution imaging spectroradiometer on terra platform," *Appl. Opt.*, vol. 47, no. 36, pp. 6796–6810, 2008.



Junqiang Sun received the B.S. degree in physics from the Changsha Institute of Technology, Changsha, China, in 1982, the Ph.D. degree in physics from the University of Science and Technology of China, Hefei, China, in 1987, and the Ph.D. degree in chemistry from the University of Florida, Gainesville, FL, USA, in 1997.

He had extensively worked in atomic and molecular physics and quantum chemistry for over a decade. He was a Principle Scientist and a Chief Support Scientist on Moderate Resolution Imaging Spectroradiometer (MODIS) and Visible Infrared Imaging Radiometer Suite (VIIRS) calibration and characterization with Global Science and Technology, Inc. (GST), Greenbelt, MD, USA, and Sigma Space Corporation, Lanham, MD, respectively. He is a Chief Research Scientist with Science Systems and Applications, Inc. (SSAI), Lanham, serving as a Team Leader for the VIIRS Characterization Support Team (VCST) to work on VIIRS instrument calibration and characterization and also serving as instruments calibration lead to work on MODIS instrument calibration and characterization.



Xiaoxiong Xiong received the B.S. degree in optical engineering from the Beijing Institute of Technology, Beijing, China, in 1982, and the Ph.D. degree in physics from the University of Maryland, College Park, MD, USA, in 1991.

He is an Optical Physicist with the NASA Goddard Space Flight Center, Greenbelt, MD, where he is also the MODIS Project Scientist and the MODIS and VIIRS Calibration Scientist. In addition to remote sensing, he had also worked in the fields of optical instrumentation, nonlinear optics, laser/atomic spectroscopy, and mass spectrometry.

Dr. Xiong is a fellow of SPIE.